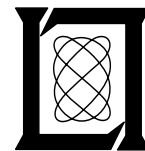# Wind Shear Detection Using the Next Generation Airport Surveillance Radar (ASR-11)

M.E. Weber

12 July 1999

Lincoln Laboratory

MASSACHUSETTS INSTITUTE OF TECHNOLOGY

LEXINGTON, MASSACHUSETTS

1. Report No. ATC-266	2. Government Accession No.	3. Recipient's Catalog No.
4. Title and Subtitle Wind Shear Detection Using The Next Generation Airport Surveillance Radar (ASR-11)		5. Report Date 12 July 1999
		6. Performing Organization Code
7. Author(s) Mark E. Weber		8. Performing Organization Report No. ATC-266
9. Performing Organization Name and Address MIT Lincoln Laboratory 244 Wood Street Lexington, MA 02420-9108		10. Work Unit No. (TRAIS)
		11. Contract or Grant No. DTFA01-93-Z-02012
12. Sponsoring Agency Name and Address Department of Transportation Federal Aviation Administration Washington, DC 20591		13. Type of Report and Period Covered Project Report
		14. Sponsoring Agency Code

15. Supplementary Notes

This report is based on studies performed at Lincoln Laboratory, a center for research operated by Massachusetts Institute of Technology, under Air Force Contract F19628-95-C-0002.

16. Abstract

The Federal Aviation Administration (FAA) is deploying a Weather Systems Processor (WSP) for the current-generation Airport Surveillance Radar–ASR-9. The WSP performs Doppler wind measurements, then automatically detects low altitude wind shear phenomena, tracks thunderstorm motion, and displays appropriate graphical and alphanumeric alerts to air traffic control (ATC) personnel. The FAA and U.S. Air Force are now procuring an ASR-11 to replace older terminal surveillance radars at facilities that did not receive the ASR-9. The ASR-11 differs from the ASR-9 in its use of a low peak power solid state transmitter, a pulse-compression receiver, and short (five-pulse) pulse bursts at both different pulse-repetition frequencies (PRF) and different RF frequencies.

In this report, we assess the technical and operational issues associated with adding a WSP to the ASR-11. The existing WSP data processing and display technology are largely re-usable for the ASR-11 based WSP. Ground clutter filter coefficients and the length and number of coherent processing intervals would need to be changed to conform to the ASR-11 pulse transmission strategy, and straightforward adaptations to the equations used in the pulse-pair weather reflectivity and Doppler velocity estimation would be required. With these changes, the ASR-11 could host the WSP, subject to performance degradations for low reflectivity wind shear phenomena such as dry microbursts and gust fronts.

A benefits assessment was performed to evaluate the operational requirement for an ASR-11 based WSP. Given that the FAA has already committed to deploy improved Low Level Wind Shear Alert Systems (LLWAS) at most ASR-11 airports, the incremental safety benefits for the ASR-11 WSP appear to be less than the cost of the equipment. A case can be made for deployment based on "situational awareness" benefits that the WSP has been demonstrated to provide to air traffic controllers. We estimate that the value to the public and airline industry of reductions in aircraft delay, and avoidance of unnecessary diversions, would be in excess of eight million dollars per year tallied across 18 of the larger ASR-11 equipped airports.

17. Key Words		18. Distribution Statement
Wind Shear Microburst Gust Front	Airport Surveillance Radar Weather Systems Processor ASR-11	This document is available to the public through the National Technical Information Service, Springfield, VA 22161.

19. Security Classif. (of this report) Unclassified	20. Security Classif. (of this page) Unclassified	21. No. of Pages 56	22. Price

FORM DOT F 1700.7 (8-72)   Reproduction of completed page authorized

ABSTRACT

The Federal Aviation Administration (FAA) is deploying a Weather Systems Processor (WSP) for the current-generation Airport Surveillance Radar—ASR-9. This modification exploits the coherency of the ASR-9 to perform Doppler wind measurement. Signature recognition algorithms then automatically detect low altitude wind shear phenomena, track thunderstorm motion and display appropriate graphical and alphanumeric alerts to air traffic control (ATC) personnel. The FAA and U.S. Air Force are now procuring an ASR-11 to replace older terminal surveillance radars at facilities that did not receive the ASR-9. Although the antenna pattern, scan rate and energy-on-target of the ASR-11 match the corresponding parameters of the ASR-9, two other characteristics are markedly different. It utilizes a low peak power solid state transmitter that requires transmission of long, coded waveforms and a pulse-compression receiver. Secondly, its pulse transmission sequence consists of short (five-pulse) bursts at both different pulse-repetition frequencies (PRF) and different RF frequencies.

In this report, we assess the technical and operational issues associated with adding a WSP to the ASR-11. The existing WSP data processing and display technology are largely re-usable for the ASR-11 based WSP. The following minor changes to the data processing algorithms would be required:

- Ground clutter filter coefficients and the length and number of coherent processing intervals would be changed to conform to the ASR-11 pulse transmission strategy.

- Straightforward adaptations to the equations used in the pulse-pair weather reflectivity and Doppler velocity estimation would be required.

- Parameters in the gust front detection algorithm would be adjusted to increase its ability to "extrapolate" detected gust front thin line signatures into the short-range interval where ASR-11 sensitivity to wind shear phenomena is reduced.

With these changes, the ASR-11 could host the WSP, subject to performance degradations for low reflectivity wind shear phenomena such as dry microbursts and gust fronts. A key, open technical issue is the ability to recover, by means of extrapolation, gust front detection performance in the short-range interval where ASR-11 sensitivity to wind shear phenomena is reduced owing to the low-peak power transmitter. If this can be accomplished, ASR-11 WSP performance in "moist" wind shear environments will be within the range deemed operationally acceptable for the ASR-9 based system.

A benefits assessment was performed to evaluate the operational requirement for an ASR-11 based WSP. Given that FAA has already committed to deploy improved Low Level Wind Shear Alert Systems (LLWAS) at most ASR-11 airports, the incremental safety benefits for the ASR-11 WSP appear to be less than the cost of the equipment. A case can be made for deployment based on "situational awareness" benefits that the WSP has been demonstrated to provide to air traffic controllers. We estimate that the value to the public and airline industry of reductions in aircraft delay, and avoidance of unnecessary diversions, would be in excess of eight million dollars per year tallied across 18 of the larger ASR-11 equipped airports. In addition, the FAA

may at some point choose to install ASR-11's at larger airports as an augmentation to ASR-9s, and at such airports a wind shear detection capability may be required. For this reason, it seems prudent to continue a modest engineering effort to develop the requisite technology for an ASR-11 based WSP, and to refine understanding of its expected performance.

TABLE OF CONTENTS

TABLE OF CONTENTS
(Continued)

LIST OF ILLUSTRATIONS

LIST OF TABLES

1 INTRODUCTION

Under Federal Aviation Administration (FAA) sponsorship, Lincoln Laboratory has developed a Weather Systems Processor (WSP) for the current-generation Airport Surveillance Radar—ASR-9. This modification exploits the coherency of the ASR-9 to perform Doppler wind measurement. Signature recognition algorithms then automatically detect low altitude wind shear phenomena, track thunderstorm motion and display appropriate graphical and alphanumeric alerts to air traffic control (ATC) personnel. Over the next four years, approximately 35 WSPs will be deployed to mid-density airports that did not receive the more expensive Terminal Doppler Weather Radar (TDWR).

The FAA and U.S. Air Force are now procuring another Airport Surveillance Radar—the ASR-11—to replace older terminal surveillance radars at facilities that did not receive the ASR-9. The ASR-11 provides digital aircraft track output that supports the needs of modern ATC automation systems such as the Standard Terminal Automation Replacement System (STARS). Approximately 150 ASR-11's will be procured. A contract to Raytheon Electronic Systems Division has been awarded and Government acceptance testing will commence shortly.

Raytheon's design for the ASR-11 draws heavily on an existing airport surveillance radar that they market overseas. Although the antenna pattern, scan rate and energy-on-target match the corresponding parameters of the ASR-9, two other characteristics of the ASR-11 are markedly different. It utilizes a low peak power solid state transmitter that requires transmission of long, coded waveforms and a pulse-compression receiver. Secondly, its pulse transmission sequence consists of short (five-pulse) bursts at both different pulse-repetition frequencies (PRF) and different RF frequencies.

In this report, we assess the operational and technical issues associated with adding a WSP to the ASR-11. Owing to the above differences between the ASR-9 and ASR-11, the data processing approach and performance expectations for the ASR-9 WSP do not carry over unchanged to the new radar. Section 2 addresses the operational benefits that would be realized by deployment of the WSP to airports slated to receive the ASR-11. A preliminary assessment of expected performance for a WSP operating off the ASR-11 is provided in Section 3. Key issues are the capability to suppress ground clutter without undue distortion to the weather echo spectrum, and the impact on wind shear detection of the low-peak power transmitter. Section 4 treats the data processing modifications to the WSP that would be required. Although the clutter suppression and Doppler wind estimation algorithms must be adapted to the different pulse-signaling sequence, the majority of the WSP algorithm suite carries over unchanged. In Section 5, we describe appropriate data processing and display hardware—essentially identical to that used in the ASR-9 WSP. An interface approach for providing necessary RF and timing signals from the ASR-11 to the WSP is presented. Conclusions and recommendations are given in Section 6.

2 ASSESSMENT OF OPERATIONAL BENEFITS

2.1 Previous Benefits Assessments for Ground Based Wind Shear Detection Systems

The FAA has sponsored a number of studies to quantify the operational benefits expected from deployment of terminal area weather systems. Martin Marietta Corporation led a multi-organization study to assess the effectiveness of various ground-based wind shear detection systems [1,2,3]. They considered TDWR, six-station and expanded-network Low Level Wind Shear Alert System (LLWAS), and the ASR-9 WSP. These systems were evaluated for wind shear detection effectiveness in the major U.S. climatological areas in both stand-alone and integrated configurations. Estimates for benefits to the U.S. public—through prevention of wind-shear accidents and reduction of airport delay caused by unanticipated gust-front wind shifts—were developed.

The 1991 report [2] on this cost-benefit analysis (CBA) considered some airports now slated to receive the ASR-11. These airports were served by an ASR-8 which could support a WSP owing to its highly-coherent Klystron transmitter and dual elevation receiving beams. Additional airports now scheduled to receive an ASR-11 were not considered for the WSP in this study. The ASR-7 used at these airports was deemed an unsuitable host for the WSP. As discussed below, the most recent 1994 CBA [3] updated a number of aspects of the earlier studies. This update, however, did not consider any ASR-11 sites since the FAA's strategy for replacing the ASR-7s and ASR-8s had become unclear. At that time, it was not known whether WSP was a viable option for those airports.

More recently, we have recognized that short-term forecasts of adverse weather impacts on runways or terminal-area flight routes allow for significant reduction of terminal area aircraft delay, and the prevention of some weather-related diversions. Benefits assessment conducted by Lincoln Laboratory for the Integrated Terminal Weather System (ITWS) identified more than twenty specific "benefit categories" where the information ITWS provided allowed for more effective utilization of terminal airspace during adverse weather. For each category, estimates were obtained for the number of aircraft affected and the amount of delay savings per aircraft for each thunderstorm episode. These were scaled using measurements of thunderstorm frequency and aircraft operations at each airport considered to derive an estimate for the delay that would be averted nationally through deployment of ITWS.

Rhoda and Weber [4] adapted the ITWS benefits methodology to estimate the terminal delay reduction that will be realized through deployment of WSPs at 35 ASR-9 equipped airports. Estimates of the effectiveness of the WSP product suite (relative to that of ITWS) for each benefit category were derived and some categories were excluded as not applicable at the smaller, non-hub airports where WSP will be deployed. The ITWS benefit scaling coefficients were reduced in accordance with these considerations. We also more carefully considered the mix of air-carrier, air-taxi, military and private aircraft at the WSP airports. Smaller passenger loads and airline operating costs for the latter three categories reduce the benefits realized relative to large U.S. airports where most operations involve air carriers.

In the following subsection we adapt methodologies derived in [2], [3] and [4] to derive a first order estimate of the safety and delay-aversion benefits that would accrue through deployment of WSPs at ASR-11 airports. As evidenced by the simplifying assumptions discussed below, these benefits calculations are not intended to be definitive, but rather, to provide an order of magnitude estimate of ASR-11 WSP value for comparison to its costs.

2.2 ASR-11 WSP Benefits Estimates

As noted, the 1991 CBA [2] estimated accident-aversion benefits for a number of the larger airports which have subsequently been scheduled to receive the ASR-11. Eighteen of these airports (Figure 1) qualified for the WSP enhancement based on the determination that estimated life-cycle benefits exceeded estimated costs. In the following discussion, we will consider only this subset of ASR-11 airports, since baseline estimates of the WSP's safety-related benefits are not published for the remaining sites.

Figure 1. U.S. Airports slated to receive the ASR-11. Circled sites are those qualified in an FAA cost-benefit analysis [2] for the WSP enhancement.

Our approach is to extract the accident-aversion benefits of the ASR-11 WSP from the estimates published in [2], after scaling to account for the considerations discussed below. Delay aversion benefits are calculated using the methodology of [4], together with operations counts and thunderstorm frequency data for the ASR-11 sites considered.

4

The calculations and results are summarized in Table 1. For each of the eighteen airports considered, the first two columns list respectively the projected Air Carrier and Air Taxi operations counts for the year 2000. The average number of thunderstorms per year is listed in column 3.

Table 1.
Summary of Estimated Benefits for ASR-11 WSP Deployment

Airport	Yearly A/C Ops	Yearly A/T Ops	T'stm days	Yearly Safety Ben ($K)	Yearly Delay Ben ($K)	NPV Over 20 yrs ($M)	BCR Safety	BCR Safety plus Delay
AGS	11496	22710	55	8.0	218.6	4.0	0.32	9.1
AMA	38078	7200	46	12.3	452.4	8.8	0.49	18.6
CHA	18288	24907	53	9.4	306.0	5.8	0.38	12.6
COS	38078	12838	59	28.2	596.5	12.0	1.13	25.0
CRW	19268	22440	41	10.3	241.8	4.5	0.41	10.1
FAR	10450	14610	30	10.2	99.5	1.7	0.41	4.4
FMY	78112	16802	93	42.9	1885.4	38.1	1.71	77.1
GSP	38250	18837	41	10.0	428.3	8.3	0.40	17.5
HUF	453	5521	44	13.6	16.9	0.1	0.54	1.2
LIT	58164	12905	54	31.3	816.2	16.4	1.25	33.9
MLU	8992	15040	59	8.0	175.6	3.2	0.32	7.3
PNS	32940	16118	65	15.3	584.5	11.5	0.61	24.0
ROA	25005	35498	37	6.7	294.7	5.5	0.27	12.1
SAV	38510	6022	63	18.0	622.7	12.3	0.72	25.6
SGF	7361	31817	54	8.4	183.2	3.3	0.34	7.7
STT	10427	107975	41	9.4	323.4	6.2	0.38	13.3
TLH	32619	32785	83	22.7	807.5	16.1	0.91	33.2
TRI	10448	29374	44	6.4	177.8	3.2	0.26	7.4
				Total 271	Total 8231	Total 161	Overall 0.60	Overall 18.9

The fourth column is our ASR-11 WSP "safety" benefit estimate. This was derived by scaling the benefits calculated in [2] to account for the following considerations.

(1) *Removal of Benefit Contribution from Gust Front Prediction:* The FAA CBA's [2,3] included a benefit contribution from reduced taxi-out and airborne delay associated with the WSP's ability to anticipate gust front wind shifts at the airport. This amounted to 27% of the total benefit attributed to WSP. Since we account for the wind shift prediction benefit separately, this contribution is removed from the estimates provided by [2].

(2) *Updates to CBA Methodology:* The 1994 wind shear systems CBA [3] updated the earlier analysis in three aspects. The value of human life and injury was revised to reflect current Government guidelines. For example, the value of life was increased from $1.5M to

$2.5M. Aircraft operations count projections for candidate WSP airports were updated over the period of benefits analysis (2000-2020). Finally, a more careful analysis of the effects of airborne wind shear detection systems in reducing the "safety benefits pool" was included. This pool is the costs associated with accidents expected to occur in spite of the wind shear detection technology and avoidance/recovery procedures already in place. The reductions accounted for:

- A determination that pilot awareness of wind shear phenomena had increased in recent years;

- Improvements in wind shear recovery training and newer, more powerful aircraft that facilitate successful recovery;

- Recognition that the commercial aircraft fleet was making increasing use of airborne wind shear detection equipment.

Overall, the considerations in this update resulted in a net 16% increase in the safety benefits estimates for the WSP. Since ASR-11 airports were not considered in this updated CBA, we have scaled the earlier safety benefits by 1.16 to account for the revised assumptions and methodology in the most recent FAA-sponsored CBA.

(3) *Technical Differences between ASR-11 and ASR-9:* In Section 3, we examine the ASR-11's effectiveness for detecting microbursts in "wet" and "dry" environments, and for detecting gust fronts. Relative to the ASR-9, we estimate that detection probabilities will be reduced by factors of respectively 0.95, 0.75 and 0.3. Reference [2] assumes that eight-tenths of aircraft accident exposure is due to microbursts and two-tenths to gust fronts. The overall reduction of ASR-11 accident aversion effectiveness is therefore 0.8—relative to an ASR-9—in a wet microburst environment, and 0.65 in a dry microburst environment. Amarillo and Colorado Springs are taken as "dry" environments. Microbursts at the remaining airports in Table 1 are assumed to be predominantly wet.

(4) *Upgrades to LLWAS at ASR-11 Sites:* Finally, we account for the reduction in the safety benefits pool associated with deployment of improved six-station LLWAS to these airports. A decision to move forward with LLWAS upgrades at smaller airports was finalized several years ago owing to lack of knowledge at that time as to the specific design of the ASR-11 and whether it would support a WSP. At the smaller airports under consideration here, we estimate that the improved LLWAS can provide detection capability approximately equal to that of the WSP over the runways. In addition, for some fraction—say, three-fourths—of the approach/departure corridors involved, LLWAS coverage will in fact extend one nautical mile out from the runway thresholds. FAA and airline industry experts have determined that the areas of wind shear risk extend three miles from the runway thresholds on approach and two miles out on departure.

Thus, the presence of an upgraded LLWAS at these ASR-11 airports reduces the safety benefits by a factor:

$$\text{Benefits Pool Reduction} = 1.0 - \{0.75 \times [1+2+1]/[3+2+2] + 0.25 \times [2]/[3+2+2]\}$$

$$= 0.46 \tag{1}$$

Here, the terms in square brackets account for LLWAS' coverage area relative to the total area of wind shear risk. We assume that the runways are 2 nmi long on average.

Delay benefits are listed in the fifth column. These are derived using the considerations of [4]. All of the ASR-11 airports considered are "non-hub" airports. For air carriers and air taxis at non-hub airports, the benefits scaling coefficients derived in [4] are respectively 0.249 and 0.049 dollars per operation per thunderstorm day. Note that, as in [4], we do not tally potential benefits that would be realized by General Aviation and military aircraft at these airports. Also, we have not adjusted the benefit coefficients to account for differences in WSP performance, most notably in the area of wind shift prediction, where the ASR-11 will be less capable.

Total "Net Present Value (NPV)," the difference between life-cycle benefits and costs, is listed in column 6 for each airport. Costs of $500,000 per site associated with WSP deployment and operation are assumed as in [3]. Column 7 lists benefits to cost ratio (BCR) treating the safety related benefits only. Column 8 gives the BCR including both safety and delay-aversion benefits.

2.3 Discussion

If both safety and delay benefits are considered, the estimated value to the U.S. public of an ASR-11 based WSP is substantial. For the eighteen airports considered, benefits exceed costs by over $150M over the 20 year life cycle considered and the associated ratio of benefits to costs is nearly 20. More than 95% of these benefits are realized through the anticipated ability of air traffic controllers and pilots to utilize the WSP products to reduce the amount of aircraft delay incurred during adverse weather and to prevent unnecessary diversions.

However, given current FAA budget restrictions and priorities, safety related benefits are probably most pertinent for the smaller airports slated to receive the ASR-11. Table 1 shows that the argument for deployment of WSPs to ASR-11 sites is weak if accident aversion is the key consideration. Owing to the depletion of the available benefits pool by deployment of LLWAS to these airports, only three of the airports considered exhibit safety benefits in excess of the estimated costs of WSP deployment. Our cost estimate did not include non-recurring engineering that would be associated with development of interface hardware between the WSP and the ASR-11 and modification of data processing software to account for its pulse-signaling strategy and solid-state transmitter. Inclusion of these costs would likely eliminate economic justification for deployment of the WSP modification to a small number of sites, if only safety benefits are considered.

At the current time, the long-term FAA strategy for deployment, maintenance and upgrade of terminal radars is not clearly defined. The ASR-9s are on average half-way through their

7

nominal twenty-year operational lifetime. Terminal Doppler Weather Radars have exhibited unanticipated reliability problems that bring into question their ability to meet FAA availability standards without some form of backup wind shear detection system. It is certainly possible that the FAA will at some point choose to install ASR-11's at larger airports as an augmentation to ASR-9s, and that at such airports a wind shear detection capability may be required. For this reason, it seems prudent to continue a modest engineering effort to develop the requisite technology for an ASR-11 based WSP, and to determine the expected performance. The following sections discuss our initial efforts in these areas.

3 TECHNICAL CHALLENGES AND PERFORMANCE EXPECTATIONS

Wind shear detection using the ASR-11 must confront essentially all of the technical issues that have been addressed in our earlier development and validation of an ASR-9 based WSP. On top of these, the ASR-11 pulse signaling strategy and low peak-power transmitter result in additional challenges for reliably measuring the reflectivity and Doppler velocity signatures of low altitude wind shear phenomena. In this section, we discuss these technical challenges and provide preliminary estimates of the likely performance of an ASR-11 based WSP.

3.1 Fan-Shaped Antenna Elevation Beam

The ASR-11 antenna beam patterns are essentially identical to those of the ASR-9. Figure 2 plots the high and low elevation beam patterns of the radar. In the absence of a WSP, all processing functions (aircraft detection and weather reflectivity measurement) are accomplished using the high beam at ranges less than about 15 nmi, and the low beam thereafter. An ASR's 1.4 degree azimuth beamwidth is well-matched to weather surveillance requirements. However, the fan-shaped elevation beams—5 degree half-power beamwidth with a slow "cosecant-squared" fall-off above the nose of the beam—introduce several major complications.
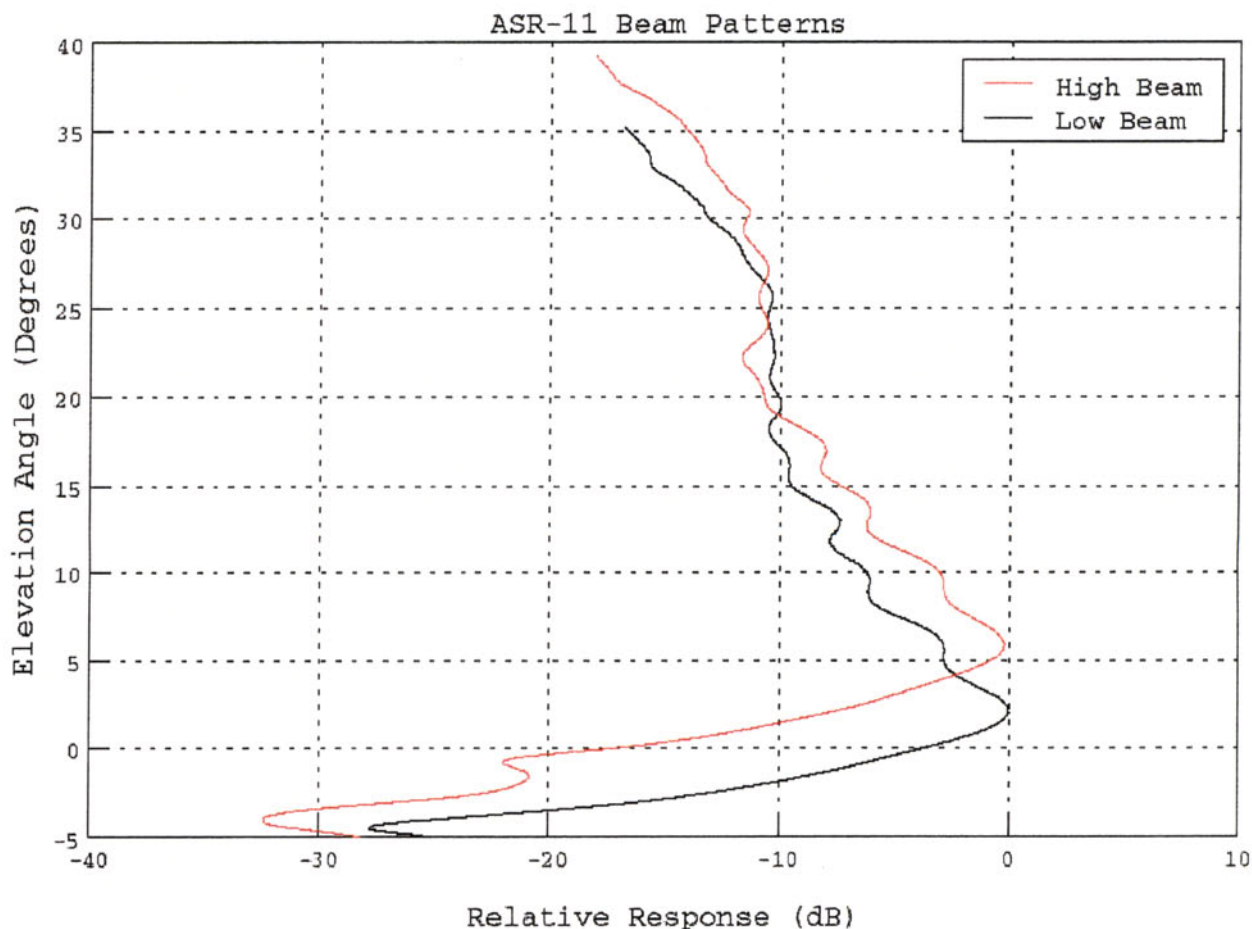

Figure 2. ASR-11 antenna elevation gain patterns.

9

Antenna gain associated with this beam pattern is approximately 34 dB, 10 to 15 dB less than that of a typical pencil beam weather radar. This reduces an ASR's capability to measure wind shear signatures not associated with precipitation, such as "dry" microbursts and gust fronts. The WSP maximizes sensitivity to low reflectivity wind shear phenomena through use of a wide dynamic range receive path that largely eliminates the need for attenuating elements such as sensitivity time control (STC) or automatic gain control (AGC). The ASR-9 based WSP has sensitivity such that 0 dBz beamfilling weather at a range of 23 km returns power equal to system noise. Most wind shear events are associated with reflectivity in excess of 0 dBz so that system sensitivity is a significant issue for the ASR-9 WSP only in arid environments such as the southwestern United States. As discussed below, sensitivity is a much greater concern for the low peak-power ASR-11.

Radar detection of microburst and gust front wind shear relies on signatures manifest primarily in the lowest few hundred meters of the atmosphere (for example, the divergent surface outflow winds that surround the microburst downdraft). An ASR's elevation beams illuminate this altitude interval, but also receive interference from higher altitude scatterers. This interference, often exhibiting a markedly different Doppler velocity, may wash out the signature of the low altitude wind shear if conventional weather radar mean Doppler estimation algorithms are employed. The WSP utilizes signals acquired near-simultaneously from the high and low beams to cancel the contribution from higher elevation angle scatterers. This approach is applicable without modification to the ASR-11.

Finally, the fan-beamed ASR illuminates ground targets more strongly than does a pencil-beam weather radar. The need to process low-beam signals at short range—where ASRs normally process only high beam returns—exacerbates this ground clutter interference. Doppler high-pass filters are used to suppress the ground clutter. In areas of strong clutter returns, however, intrinsic instabilities in the radar transmit and receive paths may prevent these filters from driving the output clutter "residue" power to or below that of system noise. Detection performance against dry wind shear phenomena in such areas may be limited by the clutter residue rather than system noise.

The stability of the ASR-11 transmit/receive chain is expected to be approximately equal to that of the ASR-9. Thus, clutter residue levels will be similar to those of the ASR-9 if the high-pass filters are designed appropriately. However, because an ASR-11 based WSP will be constrained to very short coherent processing intervals (CPI), the transition bands between the low-Doppler notches and the filter pass-bands will be significantly broader than can be realized utilizing the longer CPIs available from the ASR-9. This will increase the amount of weather spectrum distortion caused by the clutter suppression process, and may adversely affect wind shear detection capability.

3.2 Pulse Transmission Sequence

The ASR-11 transmits pulses in blocks of five, followed by a shift in both RF and pulse repetition frequency. The RF frequency diversity increases incoherent processing gain for the aircraft detection processor. The PRF diversity reduces aircraft "blind speeds" and allows for removal of out-of-trip weather and target returns. As shown in Figure 3, the radar cycles through a sequence of four transmit frequencies and PRFs. These occur in an interval approximately

equal to that required for the antenna to scan through one azimuth beamwidth. In contrast to the ASR-9, the transmitted burst sequence is not registered to antenna azimuth by means of "fill pulses."

	PRF 1	PRF 2	PRF 3	PRF 4

Short Pulse →
Long Pulse →

Transmit Frequency:

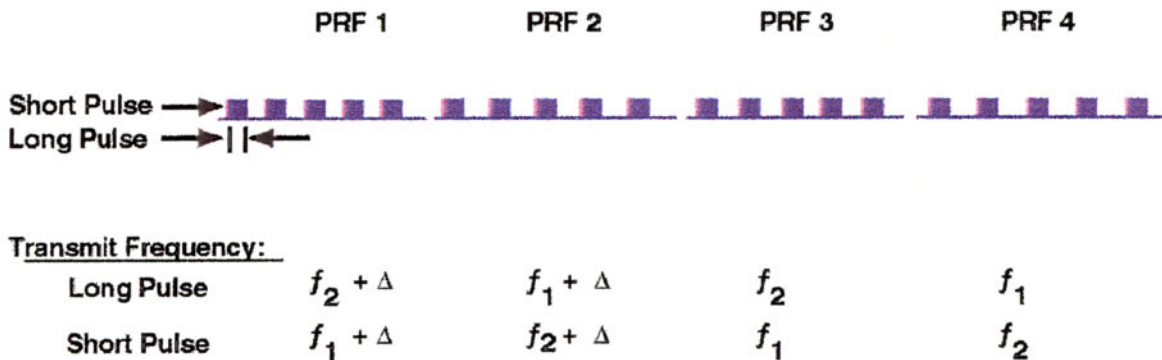|	PRF 1	PRF 2	PRF 3	PRF 4
Long Pulse	$f_2 + \Delta$	$f_1 + \Delta$	f_2	f_1
Short Pulse	$f_1 + \Delta$	$f_2 + \Delta$	f_1	f_2

Figure 3. ASR-11 pulse transmission sequence (courtesy of Raytheon ESD).

The major effect of this pulse sequence relative to WSP is the constraint it places on the CPIs available for ground clutter filtering and Doppler velocity estimation. Although we have developed techniques for coherently processing across the ASR-9's PRF transitions [5,6], the ASR-11's change in RF frequency de-correlates weather returns, thereby eliminating this option. As noted above, clutter filter transfer functions will be adversely affected by this constraint.

The absence of precise scan-to-scan azimuth registration introduces a secondary issue. The WSP algorithms for clutter suppression make use of high-resolution clutter residue maps that are used to select the appropriate filter for each range gate. The manner in which these maps are generated and used will need to be modified slightly to account for this lack of registration.

3.3 Solid State Transmitter

The ASR-11 uses a bank of solid state amplifiers to generate its transmitted RF pulse. This technology limits peak power significantly relative to that of the Klystron-amplified ASR-9. To compensate, the ASR-11 transmits a frequency modulated "long pulse," of tens of microseconds duration; a pulse-compression receiver recovers the energy on target so as make up for the reduced peak power. Out to a range corresponding to the duration of the long pulse, however, the pulse compression waveform is not usable (the transmitter is still firing). A short pulse at an offset RF frequency provides surveillance and weather data out to this range and the radar's minimum detectable signal level is reduced accordingly.

The reduction of sensitivity at ranges less than this short-to-long pulse transition has significant performance implications for the WSP since the area of operational concern for wind shear detection with an on- or near-airport ASR lies predominantly within this radius. As noted above, sensitivity for "dry" wind shear phenomena is already problematic owing to the low-gain antenna used by ASRs.

Pulse compression introduces low-level time sidelobes in the receiver output response. For the ASR-11, these vary from –40 dB to –55 dB, depending on the range at which the pulse compression receiver is operating. For intense precipitation echoes exhibiting high spatial

gradients, these sidelobes can smear areas of reflectivity spatially or introduce "images" that could occasionally trigger false detections by the WSP's meteorological algorithms. We considered this issue in detail in [7].

3.4 Performance Expectations

(a) Effect of Reduced Sensitivity

Of the issues considered above, those with the largest impact on ASR-11 wind shear detection are reduced sensitivity to wind shear phenomena at short range and the broader notches associated with the Doppler high pass clutter filters. Reference [7] describes an approach for assessing the impact of ASR sensitivity on wind shear detection. Calculation of minimum detectable weather reflectivity versus range is performed, including SNR requirements for accurate Doppler velocity measurement and the "loss" associated with partial filling of the ASR elevation beam by the meteorological target. This sensitivity profile is then convolved with measured distributions of low altitude wind shear reflectivity to compute the fraction of the wind shear events that would return adequate signal power. In this analysis, we treat microburst reflectivity distributions in "wet" (Orlando, FL) and "dry" (Denver, CO) environments, and a gust front reflectivity distribution generated by combining measurements from several locations across the U.S. The data used in these calculations are shown in Figure 4.
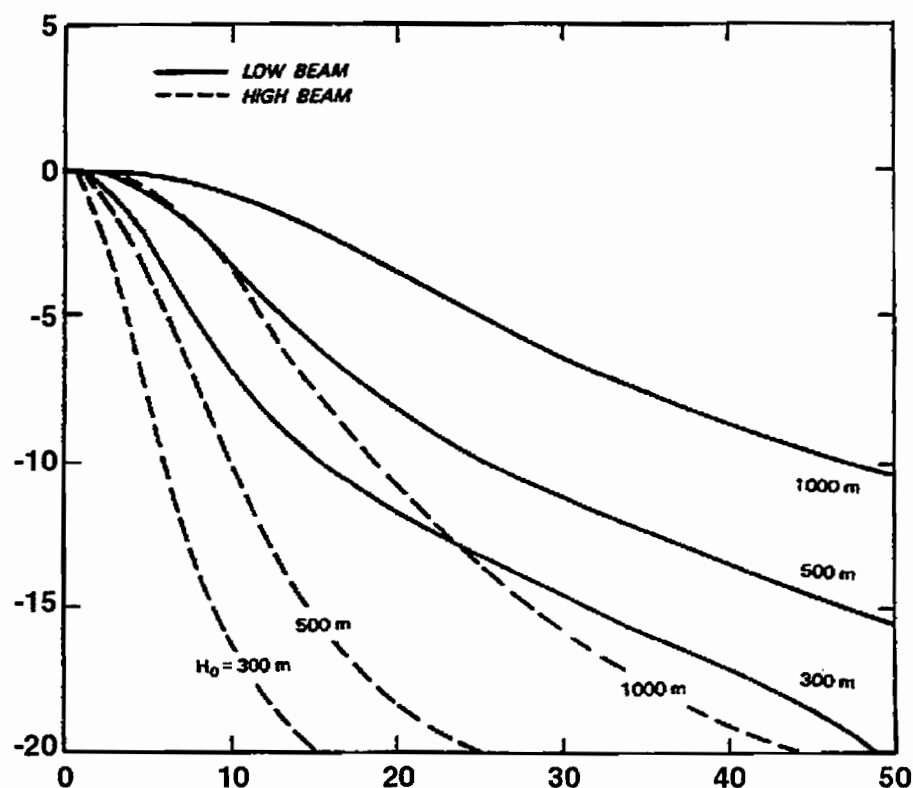
Figure 4(a). Figures (a) through (c) show data used in calculation of expected ASR-11 wind shear detection performance. Above, figure (a) shows ASR beamfilling loss versus range and outflow depth.
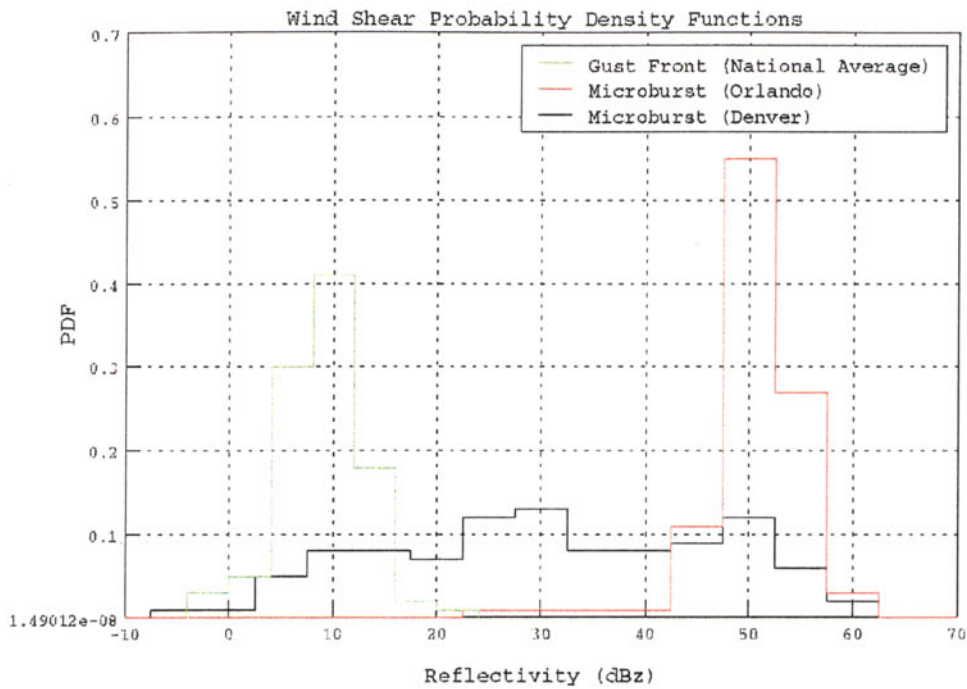
Figure 4(b). Probability density functions (PDF) of microbursts and gust fronts measured with Lincoln Laboratory TDWR testbed. Microburst data representative of a "wet" outflow environment are from Orlando, FL. Data representative of a "dry" outflow environment are from Denver, CO. The gust front distribution is a composite of measurements from Orlando, Denver, and Kansas City, KS.
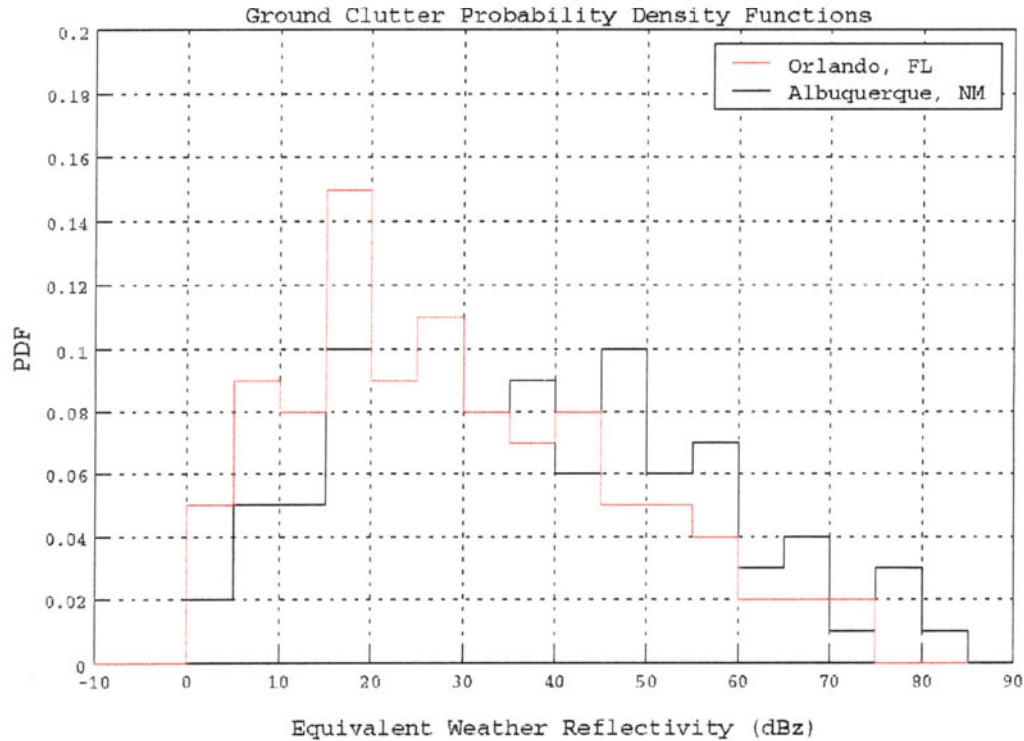
Figure 4(c). Distribution of ground clutter equivalent weather reflectivity measured with Lincoln Laboratory ASR-9 testbed in moderate (Orlando, FL) and severe (Albuquerque, NM) clutter environments. Data are from resolution cells within 30 km of the radar.

Table 2 summarizes the analysis using parameters for the ASR-9 and ASR-11. The range-interval of operational concern is taken to be 15 km. For the most extreme case, the gust front reflectivity distribution, the ASR-11's reduced sensitivity at short range results in more than a 50% lowering (relative to the ASR-9) of the fraction of wind shear events where adequate SNR would be achieved.

Table 2.
Range-Averaged (0-15 km) Fraction of Wind Shear Events
Exhibiting SNR in Excess of 6 dB

Wind Shear Reflectivity Distribution	ASR-9	ASR-11
Microburst (Wet Environment)	1.0	1.0
Microburst (Dry Environment)	0.80	0.63
Gust Front	0.82	0.38

Note that for microburst detection, both the high and low receiving beams must receive power in excess of the SNR requirement. For gust front detection, only low beam data are required. Thus significantly larger beamfilling loss is assumed in the calculations for microburst SNR (see Figure 4a). This accounts for the small ASR-9 "detection probability" decrease in a dry microburst environment relative to gust fronts, in spite of the overall higher reflectivity of the former wind shear category. For the ASR-11, the minimum detectable signal exceeds the reflectivity of many gust fronts, even with small beamfilling loss. Thus the relative dry microburst and gust front "detection probabilities" for the ASR-11 track the respective average reflectivity of the two wind shear categories.

(b) Effect of Broader Clutter Filter Notches

The data shown in Figure 4 can also be used to assess the extent to which the wider notch filters required by the ASR-11 attenuate weather returns sufficiently to prevent detection of wind shear. Figure 5 plots the transfer functions of the three high-pass filters used currently in the Lincoln Laboratory ASR-9 WSP prototype. These suppress scan-modulated ground clutter by approximately 20, 40 and 60 dB. Transfer functions for corresponding filters designed to the ASR-11's 5-pulse CPIs (see Section 4) are shown in Figure 6. For equivalent clutter suppression, the half-power width of the low-Doppler notches are roughly a factor three larger with these short CPIs.

Our analysis is detailed in Appendix A. The distribution of radial wind speeds in thunderstorm outflows (including the addition of ambient wind) determines the probability that a given clutter filter will introduce either unacceptable weather signal attenuation or will produce large Doppler velocity estimate errors due to distortion of the weather spectrum. An estimate of the frequency with which each of the clutter filters is employed is obtained using the distributions of wind shear and ground clutter reflectivity shown in Figure 4. The aggregate effect on wind shear detection performance can then be determined. Results are listed in Table 3. As with Table 2, we emphasize that the ASR-11 performance estimate should be interpreted as relative to that of a WSP operating on the ASR-9 with narrower ground clutter filters. An estimate of absolute performance for the ASR-11 is provided in the following section.
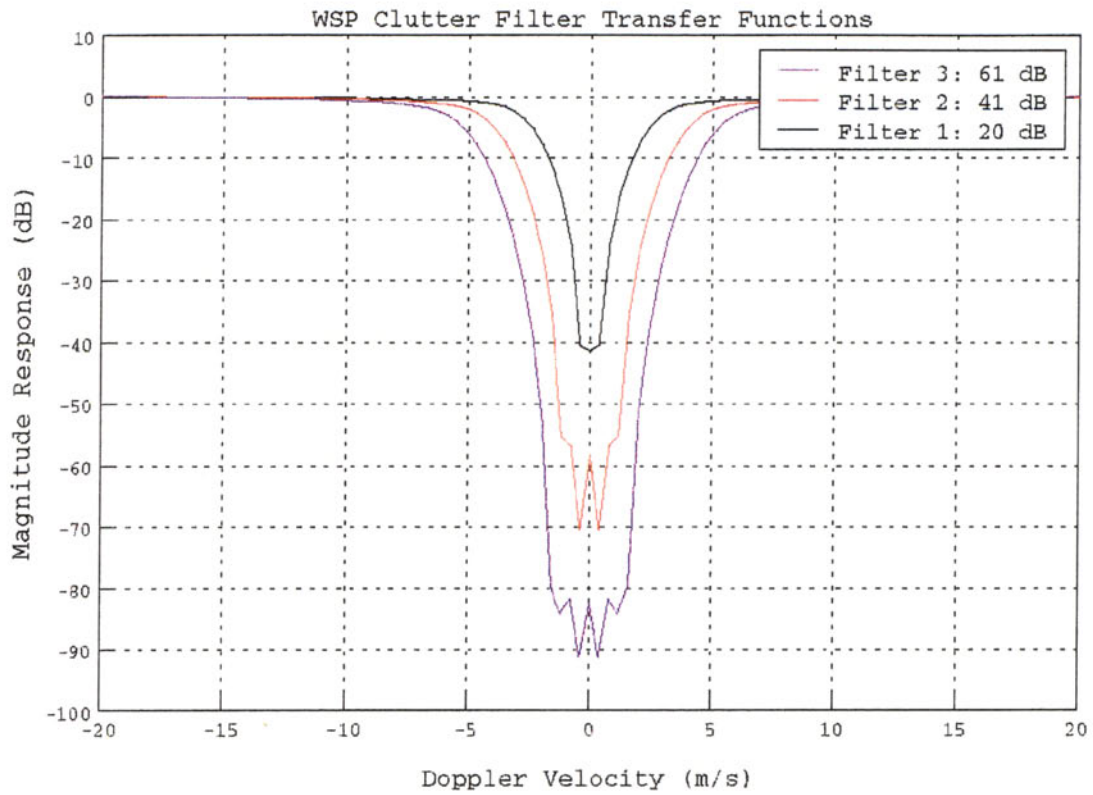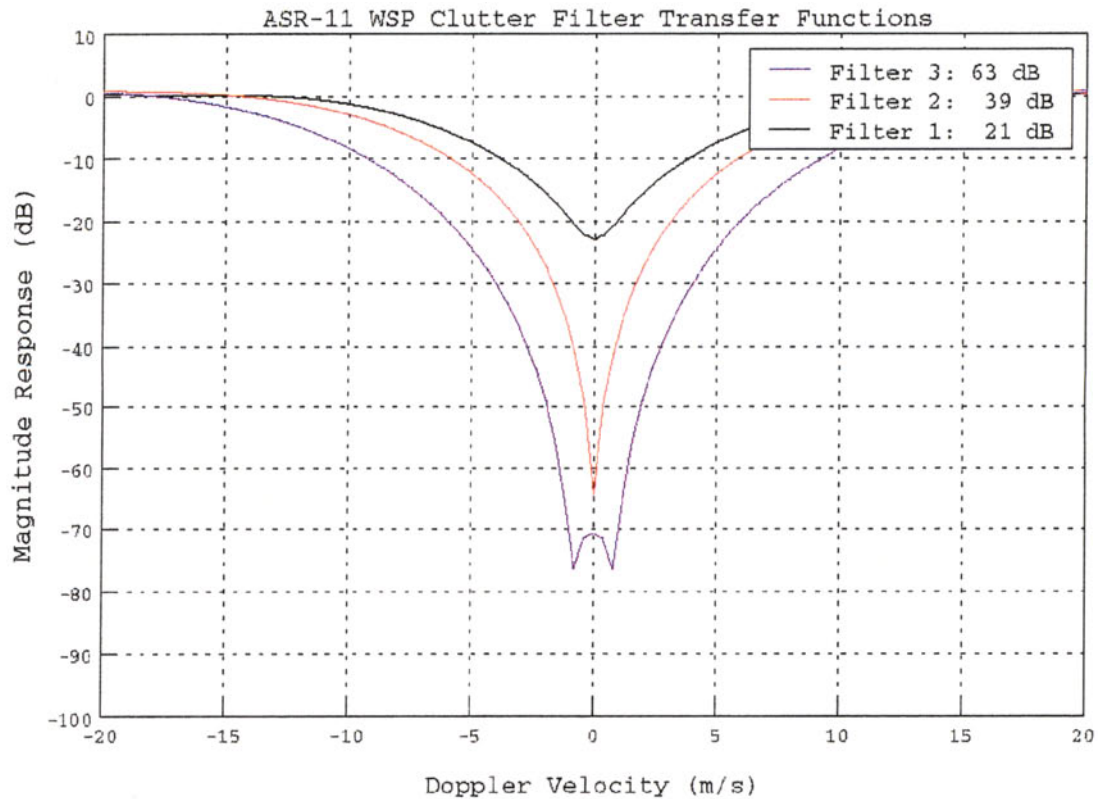
Figure 5. ASR-9 WSP clutter filter transfer functions.

Figure 6. Transfer function of WSP clutter filters designed to the ASR-11 five-pulse CPIs.

15

Table 3.
Fraction of Wind Shear Events where Clutter Filters Establish
Adequate Signal to Clutter Residue <u>and</u> Filter-Induced Reflectivity
and Doppler Measurement Biases are Acceptable

Wind Shear Reflectivity Distribution	ASR-9	ASR-11
Microburst (Wet Environment)	1.0	0.94
Microburst (Dry Environment)	0.99	0.85
Gust Front	0.92	0.53

(c) Absolute Performance Estimates

Tables 4 and 5 reproduce published [8] performance measurements for the ASR-9 WSP's microburst and gust front detection functions. The microburst statistics are based on "scoring" of data archived at four different prototype operating sites in the U.S. Performance estimates for U.S. climate regimes not directly sampled with our prototype WSP were arrived at through analysis of likely storm characteristics in these regimes.

Table 4.
ASR-9 WSP Microburst (Loss > 15 m/s) Detection Performance
within Climate Regimes (from [8])

Climate Region	Expected P_d	Expected P_{fa}
Northeast	0.85-0.90	0.10-0.15
Midwest	0.85-0.90	0.15-0.20
Southeast/Florida	0.90-0.95	0.05-0.15
South Central	0.90-0.95	0.05-0.15
Southwest	0.75-0.85	0.15-0.20
Southern California	0.85-0.95	0.10-0.15
Hawaii	0.90-0.95	0.05-0.15

Gust front performance measurements are from the most recent two sites at which the prototype has operated. Earlier data sets from the prototype are not useful for quantitative evaluation of gust front detection performance since too much sensitivity time control (STC) attenuation was used to allow for reliable detection of this phenomenon [8]. For purposes of the discussion here these statistics are sufficient for contrasting gust front detection performance in "wet" and "dry" environments.

Table 5.
ASR-9 WSP Gust Front Algorithm Detection Performance
Measured at Orlando and Albuquerque WSP Sites (from [8])

Site	P_d (gain > 10 m/s)	P_d (Gain > 15 m/s)	P_{fa}
Orlando	0.67	0.73	0.11
Albuquerque	0.50	0.74	0.11

As noted at the beginning of this subsection, we expect that the factors that would significantly reduce ASR-11 WSP performance relative to that of the ASR-9 are the former radar's reduced short-range sensitivity and broader clutter filter notches. Other performance factors, most significantly higher altitude "meteorological interference" as a result of the broad antenna elevation beams and imperfections in the data processing algorithms, are the same for the two systems and are presumably already accounted for in the statistics of Tables 4 and 5. A rough estimate of absolute performance for the ASR-11 WSP therefore can be derived by combining the results summarized in Tables 2 and 3 into an incremental "miss probability" for the ASR-11. This is then subtracted from the ASR-9 results presented above. Details of this approach are presented in Appendix B.

Table 6 summarizes these estimated incremental miss probabilities for the ASR-11 WSP. For comparison to the ASR-9 based detection statistics listed above, we assume that all microburst "Climate Regions" are wet except for the Southwest. For gust fronts, the same detection degradation must be assumed for moist and arid environments owing to our use of a "nationally averaged" gust front reflectivity distribution in deriving the performance degradation estimate. We have not attempted to estimate changes in the false alarm probability.

Table 6
Incremental "Miss Probabilities" for ASR-11 WSP
Relative to ASR-9 WSP. See Appendix B for Derivation

Wind Shear Reflectivity Distribution	Detection Probability Degradation
Microburst (Wet Environment)	0.03
Microburst (Dry Environment)	0.21
Gust Front	0.54

(d) Discussion

In wet microburst environments, ASR-11 microburst detection performance will not be significantly degraded. Relative to the performance realized on the ASR-9, the detection probability of the ASR-11 WSP will be reduced approximately 5%. Obviously, the parameters of the ASR-11 are less conducive to detection of weakly reflecting dry microburst phenomena. Integration of Table 6 with the "Southwest U.S." performance statistics in Table 4 indicates that ASR-11 WSP microburst detection probability would average about 0.6 in environments where dry microbursts occur frequently. Of the candidate ASR-11 WSP sites considered in Section 2, however, only two are likely to experience dry microbursts.

Gust front detection with the ASR-11 appears problematic in both moist and arid environments owing to the uniformly low radar cross section of this phenomenon. Taking the average gust front P_d for the ASR-9 WSP in a moist environment to be 0.7, our analysis indicates that the ASR-11 based system may detect fewer than one in five gust fronts. It is worth noting, however, that both detection issues considered in this section are most vexing at short range. The ASR-11's sensitivity to wind shear returns is the same as that of the ASR-9 at ranges beyond the short-to-long pulse transition where the long pulse is processed. Ground clutter intensity (and associated filtering requirements) also diminishes rapidly with range. Gust fronts are long-lived, large scale phenomena which may typically be detected 10 to 15 nmi before reaching the radar.

Even as they pass over the radar, gust front signatures may extend well beyond the short pulse processing range of the ASR-11. It is likely that detection probabilities could be improved by:

- Detecting, tracking and subsequently "coasting" incoming gust front signatures as they pass into the short pulse processing range;

- Extrapolating from the portion of a gust front signature that lies outside the region of reduced sensitivity and high ground clutter intensity.

Quantitative evaluation of the extent to which gust front detection performance may be improved using such extrapolation techniques is beyond the scope of this report.

4 DATA PROCESSING ALGORITHMS

The FAA and Lincoln Laboratory have invested significant resources to develop data processing algorithms for the ASR-9 WSP and have validated these through a multi-year field measurement/operational product demonstration program. Since many of the key technical challenges for the ASR-9 and ASR-11 based WSP are identical, a prudent strategy is to seek to reuse as much of the developed technology as feasible in implementing the WSP on the new radar platform. In this section, we adopt this approach to define the set of data processing algorithms required to suppress ground clutter, estimate weather reflectivity and Doppler wind fields, identify signatures associated with hazardous low altitude wind shear, track thunderstorm movement and display the information to air traffic control personnel. As will be shown, relatively few changes to the ASR-9 WSP algorithm suite (and associated software) are required to adapt to the ASR-11's parameters.

4.1 Overview

Figure 7 (from Newell [9]) is an overview of the WSP data processing software, applicable to both ASR-9 and ASR-11 algorithmic requirements. "Base data generation" encompasses the set of operations required to convert quadrature samples to reflectivity and Doppler velocity images. These images are distributed as appropriate to the "meteorological detection algorithms":

- Microburst detection algorithm;

- Machine intelligent gust front detection algorithm (MIGFA); and

- Storm motion and position extrapolation.

In addition, the base reflectivity images are smoothed and quantized into standard reflectivity intervals for display on controllers scopes and the dedicated display equipment deployed with the WSP.

Supporting the data processing algorithms are a variety of functions that facilitate data input/output, archiving, inter-process communication, product display and system monitoring/fault identification.

In the following subsections we describe the principal modifications to the ASR-9 WSP algorithms required for the ASR-11. The reader is referred to [9], [10], [11], [12] and [13] for more detailed description of the ASR-9 WSP data processing algorithms.
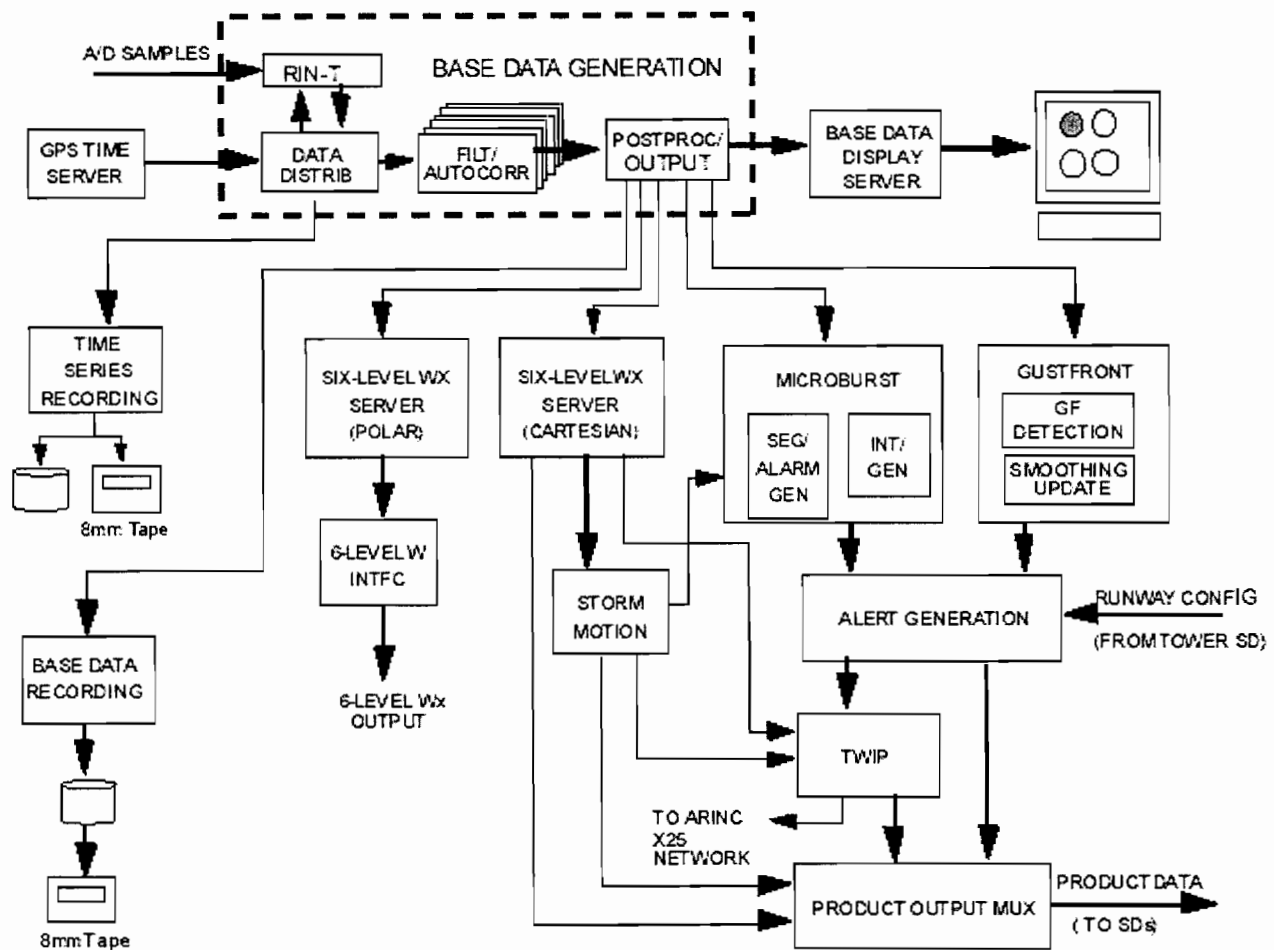
Figure 7. Overview of WSP data processing software.

4.2 Base Data Generation

These operations encompass quadrature sample ingest and scaling, ground clutter suppression, reflectivity and Doppler velocity estimation and data quality evaluation. Weber [10] documented the ASR-9 WSP base data processing algorithms, most aspects of which carry over unchanged to the ASR-11. The significant exceptions are modifications required to accommodate the ASR-11's 5-pulse CPI; these affect clutter filtering and autocorrelation function estimation.

Figure 8 shows the operations performed to compute base data. These are performed independently for each range gate and each of the 5-pulse coherent processing intervals transmitted as the ASR-11 antenna scans one beamwidth. Data from both high and low antenna beam receive paths are processed sequentially on "alternate" scans of the antenna as described in [10]. Ground clutter suppression is applied, utilizing static clutter residue maps of the ground clutter distribution to select the appropriate level of clutter suppression. The filtered echo samples are used to estimate the signal autocorrelation function at delays ("lags") equal to zero and one times each CPI's pulse repetition interval. The autocorrelation lags are stored in a recursive-averaging buffer for estimate stabilization. Base data generation is performed once per

20

antenna revolution based on the current values in this "lags buffer." Base data outputs and data quality flags are generated and passed to the meteorological detection algorithms.
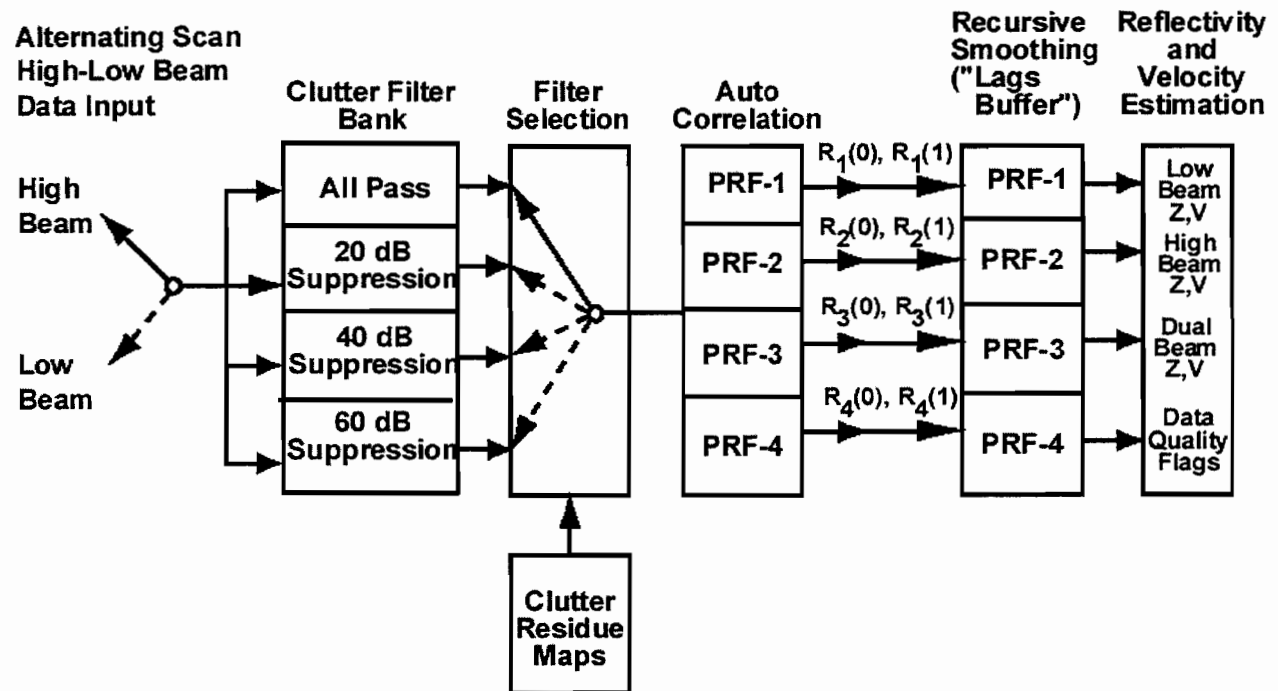
Figure 8. Overview of WSP base data processing algorithm.

(a) Clutter Suppression

The ASR-11 WSP clutter suppression filters are implemented as shift-variant linear operators applied successively to each of the 5 pulse samples in a CPI. Mathematically, this operation is accomplished by means of multiplication of the 5-sample (complex) data vector by a 5x5 real element filter matrix **H**. In matrix notation, the filter output vector Y is related to the input data vector X by:

$$Y = H\,X \qquad\qquad (2)$$

Five output samples are generated, allowing for "pulse-pair" processing to estimate weather reflectivity and Doppler velocity. This operation is the same as that used to implement ground filters in the ASR-9 WSP, except for the CPI-length. The ASR-9 WSP processes a single, 27-pulse "extended" CPI in each range cell [10]. Note that the computational requirements for clutter suppression—a significant factor in the overall processing load for the WSP—are more than a factor of seven smaller for the ASR-11 than for the ASR-9 (i.e., 4 CPIs x 5x5 real-complex multiplies per range gate versus 27x27).

The filter design technique, described by Chornoboy [14], satisfies either Chebyshev or Mean Squared Error (MSE) optimality criteria, using as input sample sequences at arbitrary, variable time spacings. In this application, the inter-pulse sampling interval is constant within a CPI.

Average magnitude responses for ASR-11 WSP clutter filters realizing nominal attenuations of 20, 40 and 60 dB were shown in Figure 6. Examples of the variation of magnitude response across the five output samples for one of the filters (filter 3) are shown in Figure 9. The first and last output pulses typically exhibit smaller signal-to-clutter improvements owing to the greater asymmetry of the input data samples. Omission of these two output samples may provide better clutter suppression performance, albeit at the expense of a 50% reduction in the already small number of pulse-pairs available for Doppler wind estimation. Trade-offs associated with this option are under investigation.
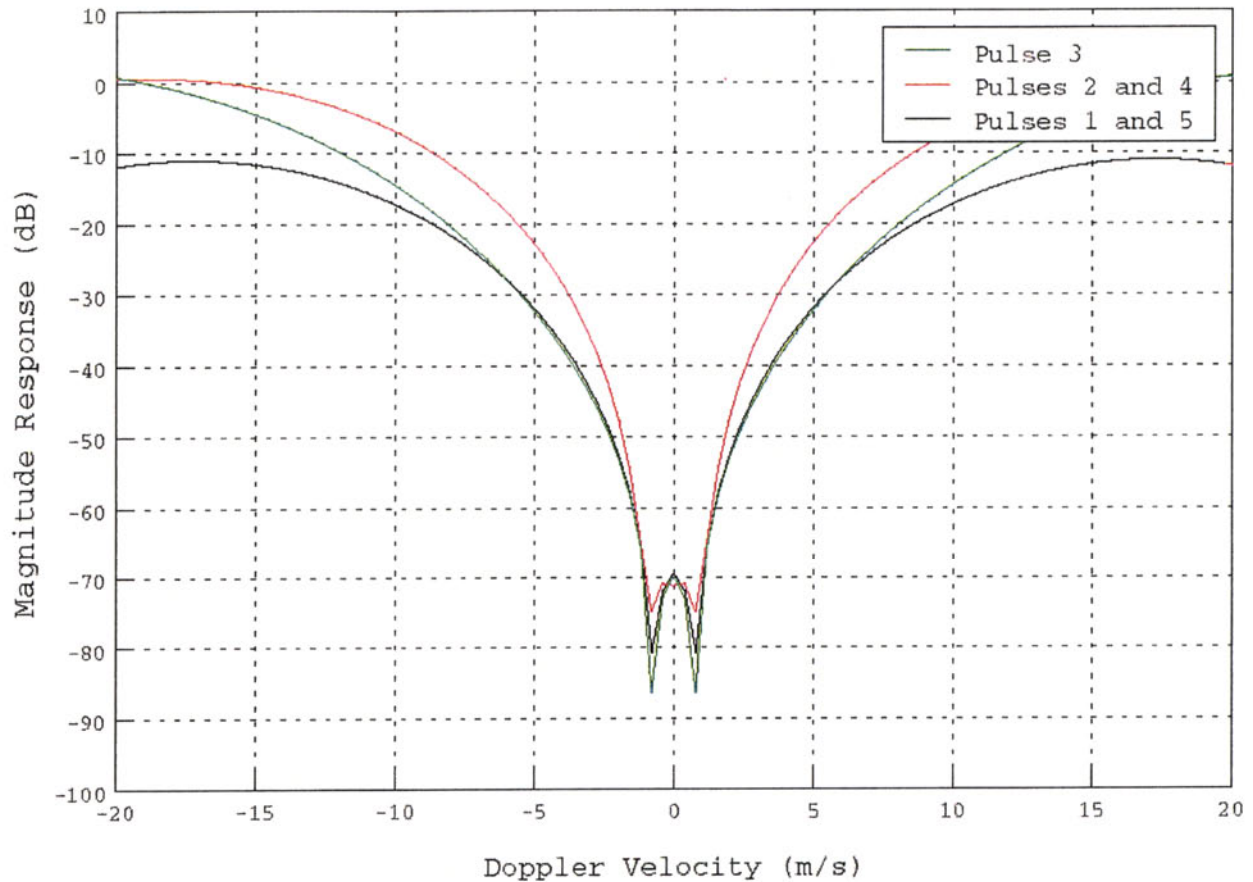
Figure 9. Individual pulse-output transfer functions for 63 dB ASR-11 WSP clutter filter.

Owing to the non-symmetrical inputs, these filters are not exactly linear phase. The resulting phase ripple produces small errors in Doppler velocity estimates. Figure 10 plots the RMS phase error (averaged across the output samples) for each of the three filters above. In their passbands, the phase errors are less than 0.1 • (corresponding to a Doppler velocity error of one-tenth the Nyquist velocity or approximately 2.5 m/s). Since both the magnitude and sign of the phase errors vary from pulse-to-pulse, they tend to cancel when Doppler estimates are performed across the CPI; thus, this RMS error is within acceptable limits.

22
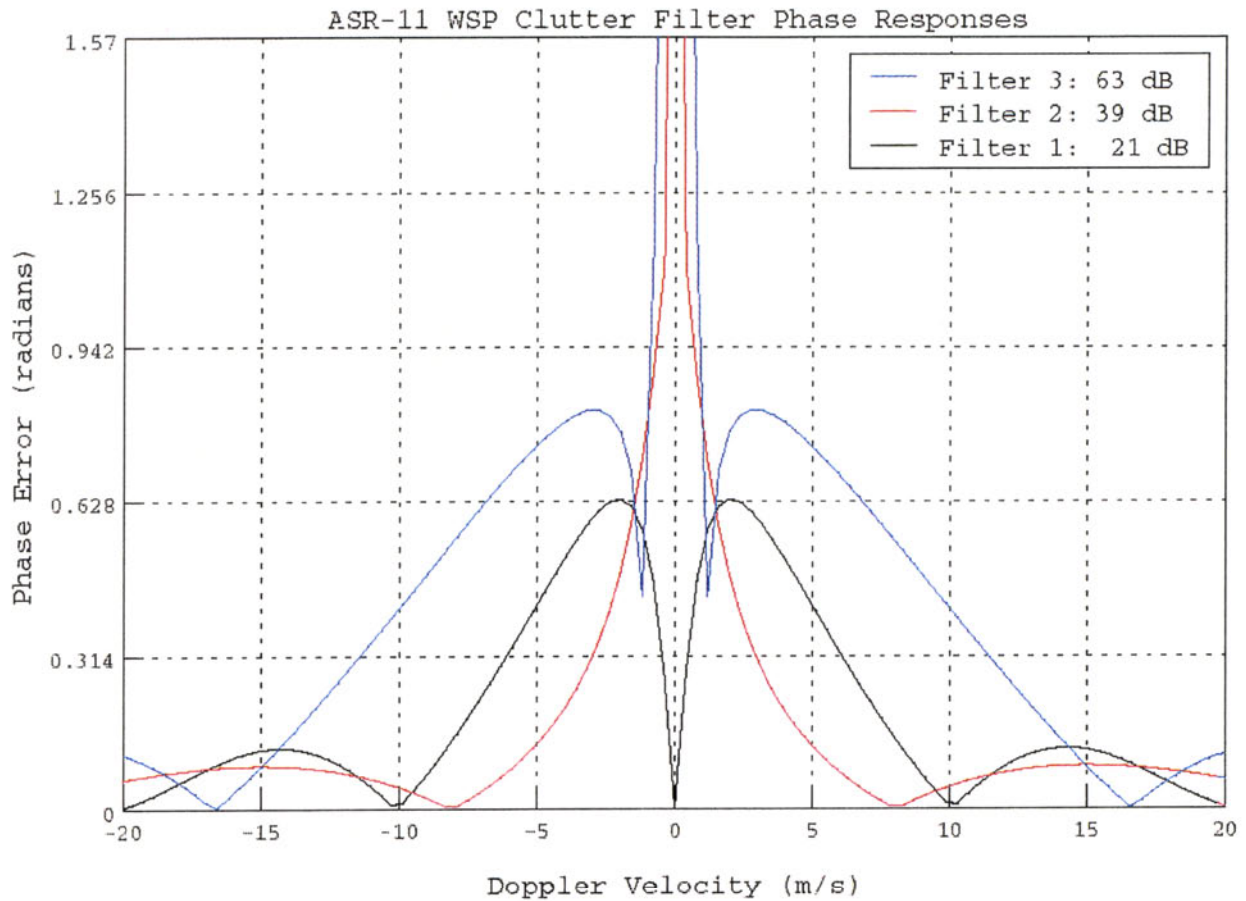
Figure 10. RMS phase error for ASR-11 WSP clutter filters.

One of the three available clutter filters or an all-pass response are selected in each range-azimuth resolution cell using clutter residue maps constructed under precipitation-free conditions. The selection algorithm chooses the least attenuating filter that provides acceptable signal to clutter residue power at its output. In contrast to the ASR-9 WSP which performs all coherent processing at the same average PRF, separate but matched clutter filter banks must be designed for each of the four ASR-11 transmitted PRFs. The clutter residue maps will be generated using appropriate combinations of the output power for corresponding filters at each PRF.

(b) Weather Reflectivity and Doppler Velocity Estimation

The signal autocorrelation function is estimated separately for each of the four CPI's using straight-forward dot product operations. Following scan-to-scan smoothing (via the aforementioned "lags buffer"), these estimates are used for measurement of weather reflectivity and Doppler velocity. Weather reflectivity is proportional to the average value of the autocorrelation function at lag-zero minus the system noise power. Appropriate consistency checks must be performed amongst the zero-lag autocorrelation magnitudes for the four CPIs in order to reject out-of-trip echoes.

23

Velocity estimation for the low and high beam received signals can be accomplished by performing a linear fit to the phase angles of the individual CPI lag-one autocorrelation measurements:

$$V(\text{beam}) = \left(\frac{\lambda}{4\pi}\right) \sum_{n=1}^{4} \phi_n(\text{beam}) \tau_n \bigg/ \sum_{n-1}^{4} \tau_n^2 \qquad\qquad \text{beam} = 1, 2 \qquad (3)$$

Here, ϕ_n is the phase angle of the lag-one autocorrelation measurement for CPI n and τ_n is the associated PRI.

The "dual beam velocity" measurement [10] used by the microburst detection algorithm isolates the low-altitude component of the received weather spectrum:

$$V(\text{dual}) = \left(\frac{\lambda}{4\pi}\right) \sum_{n=1}^{4} [\phi_n(\text{low}) - \text{weight} \bullet \phi_n(\text{high})] \tau_n \bigg/ \sum_{n=1}^{4} \tau_n^2 \qquad (4)$$

measurements, CPIs determined to be contaminated by out-of-trip returns must be eliminated from the summations in (3) and (4).

4.3 Meteorological Detection Algorithms

(a) Microburst Detection Algorithm

The WSP microburst detection algorithm consists of two principal modules (see Figure 11). The first process, "Segment and Alarm Generation," searches for candidate divergence signatures in the low altitude Doppler velocity field. A straightforward radial-by-radial search is performed for the characteristic increasing (with range) velocity signature associated with microburst outflows. The resulting "shear segments" are subjected to scan-to-scan continuity tests, grouped azimuthally and passed on to a verification process that ensures that the candidate microburst detections are physically plausible. This verification process accepts input from the second main algorithm module: a bank of image processing operators that generate an "interest image" defining areas capable of supporting microburst outflows. The operators search for:

- Reflectivity spatial structure indicative of the liquid water cores that drive microburst downdrafts;

- Temporal evolution of the reflectivity consistent with the formation and descent of these liquid water cores;

- Structural and kinematic features that can cause divergence signatures that are not microburst outflows. This class of image operator inhibits the declaration of microbursts.

Essentially all of the phenomenological and sensor-related design issues for the microburst algorithm are common to the ASR-9 and ASR-11 based WSP. Other than adjustment of certain parameters in the algorithm to account for the ASR-11's reduced sensitivity to wind shear returns at short range, we see no need for changes to this algorithm.
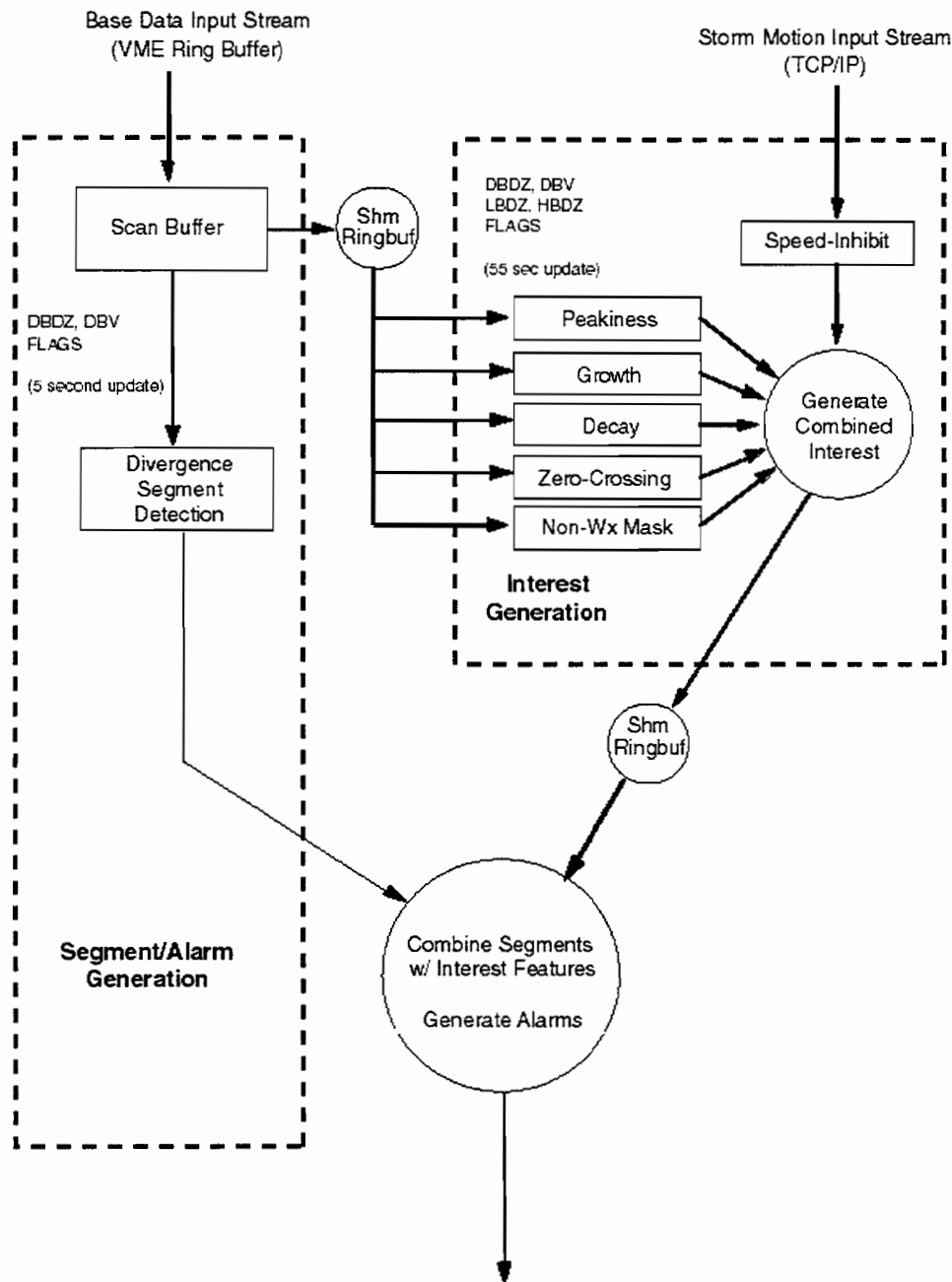
Figure 11. Overview of WSP microburst detection algorithm.

(b) Gust Front Detection Algorithm

The WSP Machine Intelligent Gust Front Algorithm (MIGFA) [12] employs multiple image processing operators that search the reflectivity and Doppler velocity imagery for features selectively indicative of gust fronts. Because an ASR's intrinsic sensitivity is often inadequate to directly measure the convergent radial velocity pattern associated with gust fronts, MIGFA's feature detectors are designed to recognize manifestations of the thin line echo along a front's leading edge. This subtle feature can be recognized as a slight increase in radar reflectivity

and/or as a line of spatially coherent Doppler velocity measurements, embedded in a noise background where gate-to-gate velocity variation is much higher. Movement of thin lines through a background of stationary ground clutter residue and slower moving storm cells often facilitates their detection.

Figure 12 is a block diagram of the WSP MIGFA. The feature detector bank as constructed for the ASR-9 WSP will be completely reusable for the ASR-11 based system. Spatial resolution and temporal updates will be identical and the characteristics of gust front signatures, where present, will be the same.

As noted, thin line signatures may be more poorly defined or absent in the ASR-11's short-pulse processing interval. Modification of MIGFA's "feature extraction" and "detection feedback" functions would facilitate extrapolation of gust front detections into this "cone of silence." Two techniques are already in place in MIGFA to accomplish this:

- A spatial ("bow-tie") filter operates on the combined interest image, just prior to the feature extraction stage, to merge gust front thin line segments that have been fragmented owing to insufficient SNR, ground clutter residue or out-of-trip weather returns;

- The Detection History that is fed back into the combined interest image pre-sensitizes the algorithm in regions where MIGFA expects the signature of a gust front that is currently under track.

More aggressive utilization of MIGFA's extrapolation features could presumably improve the ASR-11's short-range gust front detection capability. It is likely, that some associated increase in false alarm probability would occur. Implementation of a modified version of MIGFA incorporating these changes, and testing as recommended in the concluding section of this report is required to fully understand the gust front detection capability of the ASR-11 WSP.

Base Data Stream

Center Field Wind

Gust Front Detection Task

LO_DBZ, LO_VEL, HI_DBZ, HI_VEL,
DUAL_DBZ, DUAL_VEL, FLAGS
(2 min. update rate)

Scan Buffer

Feature Detection

Reflectivity Thin Lines

Velocity Variance Thin Lines

Thin Line Motion

Velocity Convergence

Non-Weather Mask

Generate
Combined
Interest

Detection History

Feature Extraction

Detection Feedback

GF Detections/Forecasts
at 2 min. update rate

Gust Front Update Task

Gust Front Update

Current GF Detections + 10, 20 min. Forecasts to SD
1 min. Update Rate

Figure 12. Overview of WSP gust front detection algorithm.

(c) Storm Motion Algorithm

The storm motion/storm extrapolated position algorithm [13] was developed originally for pencil beam weather radars and has been applied successfully to reflectivity imagery from TDWR, NEXRAD and the ASR-9. Figure 13 is a block diagram of the major processing steps. The algorithm's input is a succession of reflectivity images separated in time by one to five minutes. These images are segmented into sub-images which are cross-correlated with the

27

corresponding sub-image from the preceding scan. The peak in the cross correlation function determines the local image displacement between scans and is used to set up a gridded "motion image."

The storm analysis module contours the reflectivity image and identifies precipitation regions ("storm cells") for which motion estimates will be displayed. A speed and direction of motion estimate is assigned based on extrapolation from the grid points in the motion image. The storm extrapolated position module delineates the "leading edge" of storm cells and extrapolates this edge using the associated motion estimate.

The storm motion algorithm operates only on precipitation echoes exceeding 18 dBz and displays motion estimates only for storm cells with significant areas of echo exceeding 41 dBz. As a result, the technical differences between the ASR-9 and the ASR-11—which primarily affect low reflectivity weather processing—are immaterial to this algorithm's performance. No modifications are required to utilize the WSP storm motion algorithm for the ASR-11.
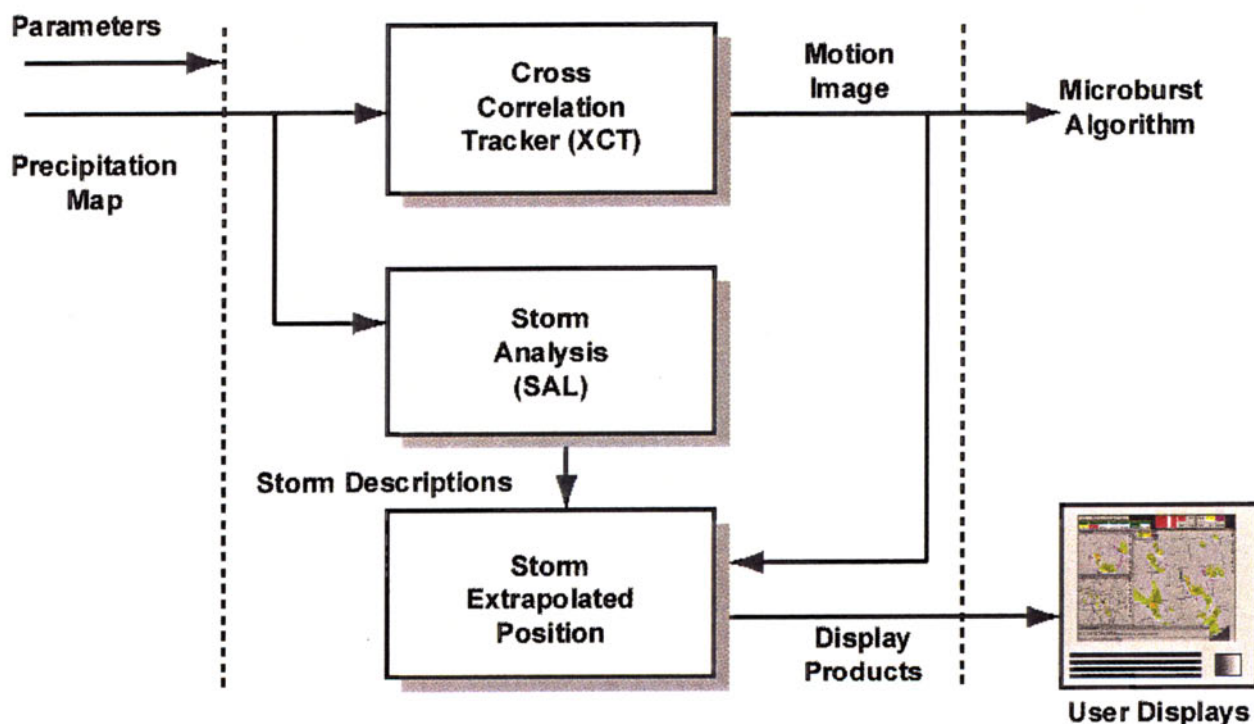

Figure 13. Overview of storm motion/storm extrapolated position algorithm.

5   PROCESSING HARDWARE AND ASR-11 INTERFACE

5.1   Data Processing and Display Hardware

The feasibility of re-using the ASR-9 WSP algorithms and software for the ASR-11 implies that the associated data processing and display hardware should be adopted as well. The FAA's strategy for ASR-9 WSP implementation relies on a high degree of reuse of the hardware and software technology employed in Lincoln Laboratory's developmental WSP. The following description of this prototype's hardware systems is adapted from [9].

A block diagram of the radar-site data processing system is shown in Figure 14. The majority of the WSP functionality is contained in a single VME chassis containing commercial-off-the-shelf (COTS) data processing cards. (The I/O board shown is the diagram is a Lincoln-built custom board but will soon be replaced by a commercially built radar interface system.) Two primary processing platforms are utilized: Intel i860 based array processors from Mercury Computer Systems for base data generation functions and SPARC-based single board computers (SBC) from FORCE Computers hosting the meteorological algorithms. A bulk memory card and GPS receiving card round out the VME board suite.
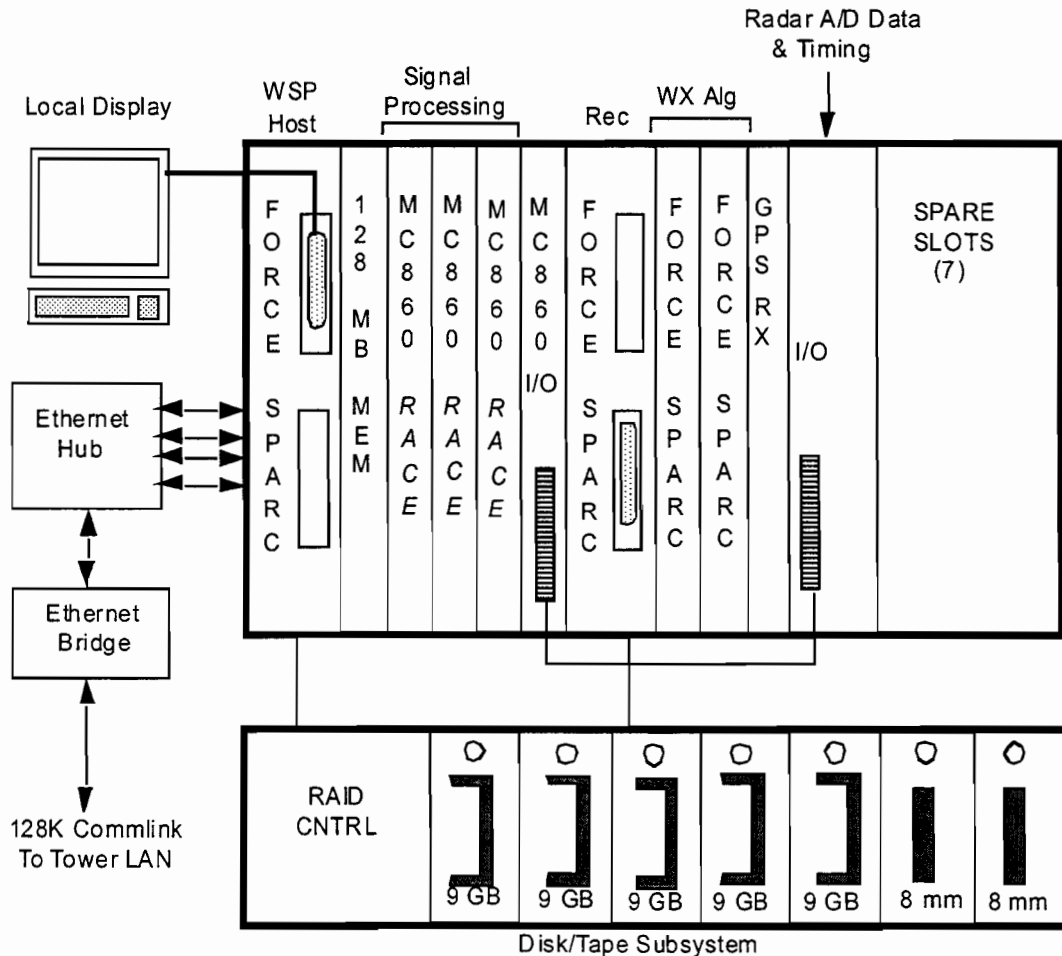

Figure 14. Block diagram of WSP data processing hardware.

29

The Mercury boards handle time-series data I/O and perform compute intensive signal processing operations. All devices on these boards are interconnected via the "RACEWay," a high speed crossbar network which allows each device network-wide shared memory access. As currently configured, the boards provide computing capacity of approximately 300 million floating point operations per second (MFLOPS). As noted, the smaller CPIs that would be processed by an ASR-11 WSP result in a reduction of ground clutter filter processing load by a factor of seven. Since the filtering operation accounts for the majority of the signal processing load, the number of Mercury boards and/or processors per board could be scaled back for the ASR-11 WSP.

The Force SBCs are used not only for meteorological algorithm processing but for data recording, automatic system monitoring/fault isolation and for system "host" functions. The FORCE card in VME slot 1 performs this host function for the Mercury boards, providing the software download process as well as allowing them to access disk/terminal I/O services. This board is equipped with a graphics card and display. It hosts the WSP's "remote monitoring functions" (RMF), the associated graphical operator's terminal and drives displays of the meteorological base data and algorithm performance monitors. These display functions coexist on separate virtual windows on the Local Display.

A typical configuration of the user display hardware at the ATCT is shown in Figure 15. This Local Area Network (LAN) is connected to the WSP VME data processor at the radar site via Ethernet bridges and a wideband communications line. SUN workstations are used for both the Air Traffic Controller "Situation Displays (SD)" and a remote operator's "Maintenance Data Terminal (MDT)." Attached to each SD via a serial connection are a number of ribbon display terminals (RDT), currently 12-line by 24 character large-format text displays from DALE Electronics.
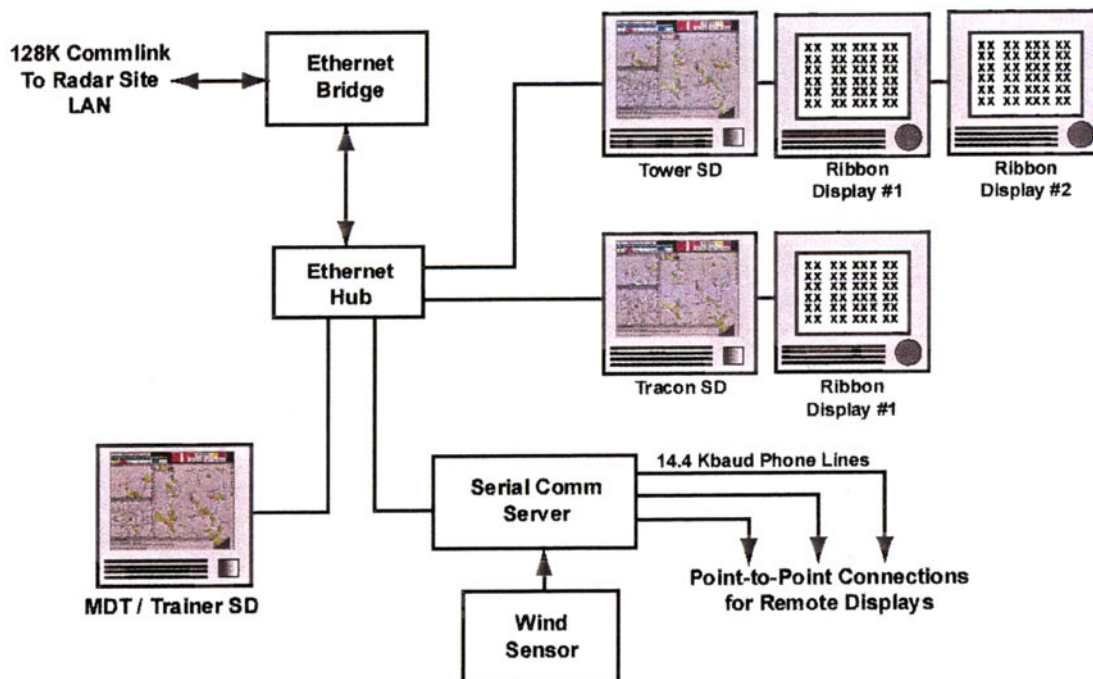

Figure 15. Typical WSP graphical and alphanumeric display hardware at ATCT.

30

5.2   WSP to ASR-11 Interface

In contrast to the WSP's data processing and user display subsystems, the hardware required to extract necessary microwave, timing and status signals from the host radar will differ in detail between the ASR-11 and ASR-9 based systems. In this subsection, we describe the likely configuration of a WSP to ASR-11 interface, based on the interface that has been developed for the ASR-9. This discussion is of a preliminary nature and is intended only to expose the major design considerations.
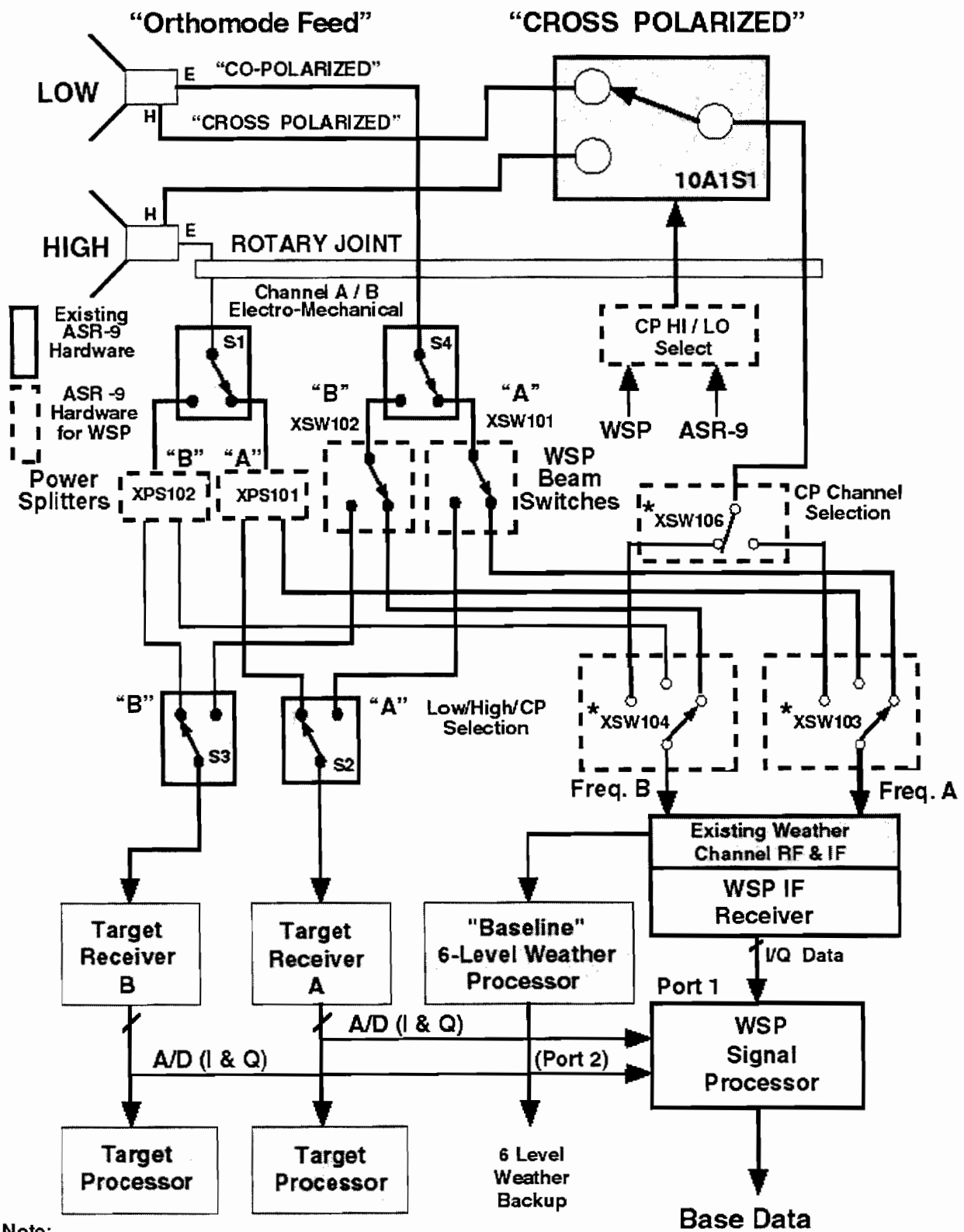
(a) Microwave Signal Access

Over the range interval of concern for wind shear detection (approximately 6 nmi for microbursts and 15 nmi for gust fronts), the WSP requires data from both high- and low receiving beams of the ASR. In addition, its receiver should provide sufficient dynamic range to support linear detection over the 70 to 80 dB range spanned by meteorological targets and ground clutter, without the use of sensitivity-reducing attenuation (STC and/or AGC). For these reasons, the WSP must extract appropriate signals from the ASR's microwave paths and must include a separate, wide dynamic range receiver.

Figure 16 is a high-level flow diagram of the RF paths that provide signals to the WSP processor. This topology is applicable to both the ASR-9 and ASR-11 based systems.

As described in [10] and [15], the network of microwave switches and couplers provides appropriate "co-polarized" and "cross-polarized" high and low beam data to the WSP receiver, as a function of the ASR's polarization mode, active channel selection, processing range and scan number. Briefly, the depicted interface element functions are as follows:

(1) 3 dB Power Dividers (XPS102 and XPS 101) for high beam signal extraction in linear polarization (LP) mode;

(2) Added microwave Beam Switches (XSW102 and XSW101) for low beam signal extraction in LP mode;

(3) Circular polarization (CP) mode signal extraction via reprogramming the existing cross-polarized microwave switch (10A1S1) to support alternate scan data collection;

(4) An RF Switch Matrix (XSW103, XSW104 and XSW106) to select amongst these paths as appropriate for the WSP receiver;

(5) A dedicated WSP IF receiver to support the system's requirements for maximum sensitivity and wide dynamic range in the operationally critical area for wind shear detection (within 15 nmi of the radar). For the ASR-11, a duplicate of the existing target and weather channel receiver, A/D converter and pulse-compression modules may provide sufficient dynamic range and sensitivity to serve this role.

31

Figure 16. Microwave signal paths for WSP.

32

(b) Digital Signal Interface: Timing, Status, Control and Target Channel A/D Extraction

The WSP requires a number of signals from the ASR timing system to synchronize its receiver and processing to the radar. These include:

(1)   coherent oscillators;

(2)   pulse transmission time;

(3)   range gate clock;

(4)   "A/B" channel on-line selection;

(5)   LP/CP mode selection;

(6)   Antenna position;

(7)   High/low beam selection.

In the case of the ASR-9 WSP, these are acquired via existing "test ports" and/or back-plane taps. The ASR-11's more contemporary, VME processor back-plane will likely facilitate access to necessary signals through the connector of a "WSP I/O" card that would be inserted in a spare slot in the ASR-11 processor card cage.

As noted above, the WSP microwave interface requires that several switches be controlled and that any attenuating devices in the receive path be reprogrammed to minimize sensitivity loss. These control functions operate based on the radar "state" (e.g., polarization, beam selection, A/B channel selection, antenna position) which in turn is defined by the signals above. The WSP-to-ASR-11 I/O card must contain simple digital logic to output control signals as appropriate.

In linear polarization mode, target channel A/D data will be required by the WSP at ranges beyond the high/low beam transition range in order to provide low beam data for the precipitation mapping and storm tracking functions. These data must be accessed via an appropriate port or bus connection in the ASR-11.

Finally, the WSP I/O card must multiplex timing and status data, target channel A/D samples and WSP receiver A/D samples and transmit these in an appropriate format to the WSP VME processor.

(c) Six-Level Weather Reflectivity "Feedback"

When the ASR-11 is in CP mode, the high-low beam switch for "cross-polarized" signals must be controlled to provide alternate scan access to each of the beams. This differs from the normal pulse-by-pulse switching which the current ASR-11 six-level weather reflectivity processor expects. When the WSP is online, responsibility for providing six-level precipitation reflectivity maps to controller's radar display equipment must be assumed by the WSP.

Alternately, the ASR-11 baseline six-level weather reflectivity processor could be adapted (via software modifications) to deal with the alternate scan beam switching.

If the WSP is to provide weather reflectivity maps to controllers' radar scopes, a "feedback" path must be implemented to provide suitably formatted precipitation maps to the ASR-11 subsystem responsible for transmission of these data. This would presumably involve an Ethernet connection into the ASR-11's computer system, with appropriate data buffering and "handshaking" between the WSP and ASR-11.

6 SUMMARY AND RECOMMENDATIONS

The analysis herein indicates that the ASR-11 could support the major wind shear detection and storm tracking functions of the Weather Systems Processor, subject to performance degradations for low reflectivity wind shear phenomena such as dry microbursts and gust fronts. A key, open technical issue is the ability to recover—via algorithm modifications—gust front detection performance in the short-range interval where ASR-11 sensitivity to wind shear phenomena is reduced owing to the low-peak power transmitter. If this can be accomplished, ASR-11 WSP performance in "moist" wind shear environments will be within the range deemed operationally acceptable for the ASR-9 based system. In arid regions, the lower average reflectivity of gust fronts and the likelihood of hazardous "dry" microburst activity precludes use of the ASR-11 as a wind shear detection sensor.

Our analysis indicates that the ASR-9 WSP data processing and display technology are largely re-usable for the ASR-11 based WSP. The core data processing software responsible for base data generation and meteorological product generation require relatively minor changes for adaptation to the ASR-11. Specifically:

(1) Ground clutter filter coefficients and the length and number of coherent processing intervals would be changed to conform to the ASR-11 pulse transmission strategy.

(2) Straightforward adaptations to the equations used in the pulse-pair weather reflectivity and Doppler velocity estimation would be required.

(3) Parameters in the machine intelligent gust front algorithm would be adjusted to increase its ability to "extrapolate" detected gust front thin line signatures into the short-range interval where ASR-11 sensitivity to wind shear phenomena is reduced.

Software required for product display to air traffic users, data archiving, algorithm monitoring, inter-process communication, system monitoring and fault isolation may be used unchanged in the ASR-11 WSP. The data processing and display hardware, and the communications networking equipment will likewise require little or no modification.

The interface between the ASR-11 and the WSP will require some new development. While the approach used for the ASR-9 based system is largely applicable, details of the hardware, firmware and software that comprise this interface will require modification. Owing to the use of modern, "open" computer systems and bus-architectures in the ASR-11, we believe that this interface will probably be more straightforward in many areas than has been required for the ASR-9.

A significant issue is the operational requirement for an ASR-11 based WSP. As analyzed in Section 2, the safety benefits for enhanced wind shear detection capability at the smaller airports slated to receive the ASR-11 are low in relation to the cost of the equipment. A case can be made for deployment based on the "situational awareness" benefits that the WSP has been demonstrated to provide to air traffic controllers. We estimated that the value to the public and airline industry of reductions in aircraft delay, and avoidance of unnecessary diversions, was in excess of eight million dollars per year tallied across 18 of the larger ASR-11 equipped airports.

The long-term FAA strategy for deployment, maintenance and upgrade of terminal radars is not clearly defined. It is certainly possible that the FAA will at some point choose to install ASR-11's at larger airports as an augmentation to ASR-9s, and that at such airports a wind shear detection capability may be required. For this reason, it seems prudent to continue a modest engineering effort to develop the requisite technology for an ASR-11 based WSP, and to refine understanding of its expected performance.

Realistic simulation of ASR-11 signals to support algorithm refinement and validation can be accomplished using data sets collected with the ASR-9 WSP testbed. These are comprised of time-series recordings of wind shear phenomena from the ASR-9, and coincident wind shear "truth" obtained through analysis of pencil beam weather radar data. ASR-11 time series data may be simulated from the ASR-9 recordings by:

(1) Extraction of five-pulse subsets of the ASR-9's eight- and ten-pulse constant PRF blocks. Multiple decorrelated realizations of these "ASR-11 CPIs" can be obtained for a given range gate using data from successive antenna scans;

(2) Addition of digital "noise" to the recorded time series data to simulate the ASR-11's reduced sensitivity within its short-pulse processing interval;

(3) Simulation of pulse-compression "range sidelobes" by convolving simulated ASR-11 base data with filters that replicate the sidelobe structure. This approach was described in [7].

An examples of an ASR-11 reflectivity and Doppler velocity image, simulated using the above techniques is shown in Figure 17. The signal processing strategy described in Section 4 has been applied to the input time series data.
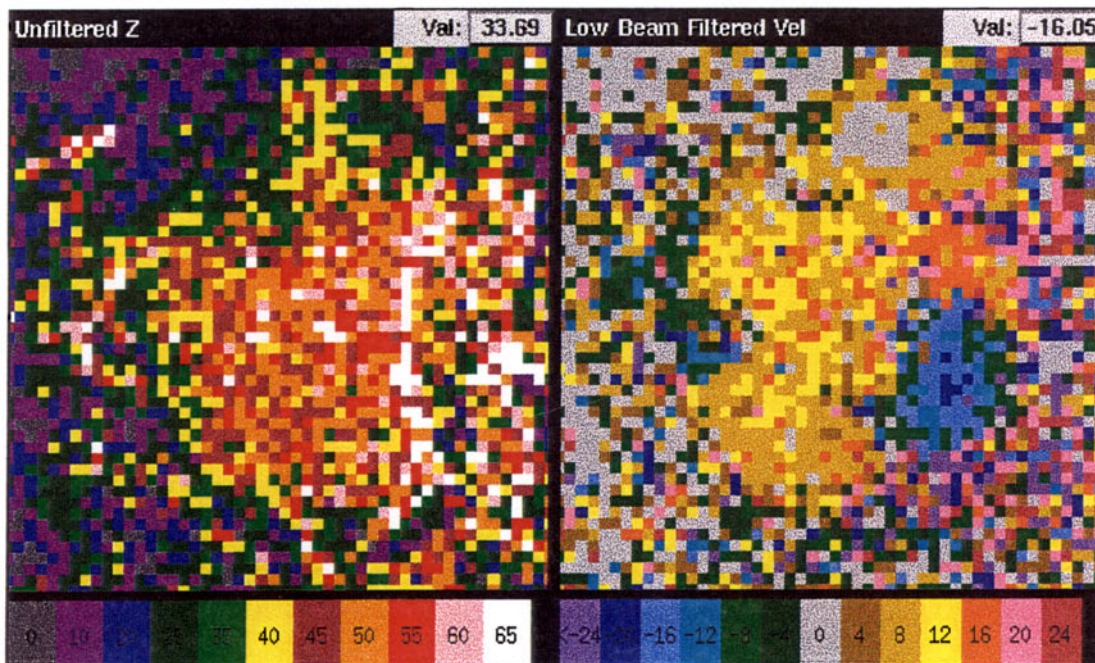

Figure 17. Example of simulated ASR-11 reflectivity and Doppler velocity measurements, using time-series data from Lincoln Laboratory's ASR-9 testbed.

The Laboratory currently operates two real-time ASR-9 WSPs prototypes on the airport at the Albuquerque, NM International Airport. One operates on the Lincoln operated mobile testbed ASR-9. As described in [8], this system has been the prime data source for development of the WSP algorithms and system design. We have recently installed a second prototype WSP on the FAA operational ASR-9 at Albuquerque which will provide operational products to Albuquerque ATC until the production WSP configuration is installed there. An efficient way to comprehensively evaluate ASR-11 WSP performance would be to implement the above simulation techniques within the testbed WSP's signal processing subsystem, along with the data processing modifications described in Section 4. Extensive, real-time data collection, analysis and performance scoring could be accomplished in conjunction with ongoing ASR-9 WSP prototype operations. Albuquerque's arid environment provides an excellent spectrum of microburst and gust front reflectivities for evaluation of performance versus wind shear cross section.

Finally, a modest effort to refine the WSP to ASR-11 interface concept would be worthwhile. Consultation with Raytheon engineers familiar with the ASR-11 system could flesh out the major interface questions in short order. Alternatively, access to an ASR-11 and system documentation would allow the Lincoln Laboratory engineers who developed the ASR-9 WSP interface to delineate the appropriate strategy.

APPENDIX A

PERFORMANCE IMPACT OF CLUTTER SUPPRESSION FILTERS

A key input to the following analysis is the distribution of wind speeds in microbursts and gust fronts. Figure A-1 summarizes differential velocities for a large fraction of the microbursts observed over seven years operation of the FAA/Lincoln Laboratory TDWR testbed at various U.S. locations. The distribution of differential velocities for most years is approximately exponential. (During the first two years of testbed operations, the relative inexperience of the site personnel who performed this analysis reduced the number of identified low-velocity microbursts. For this reason, we discount the observations from 1986 and 1987 in the following analysis.)
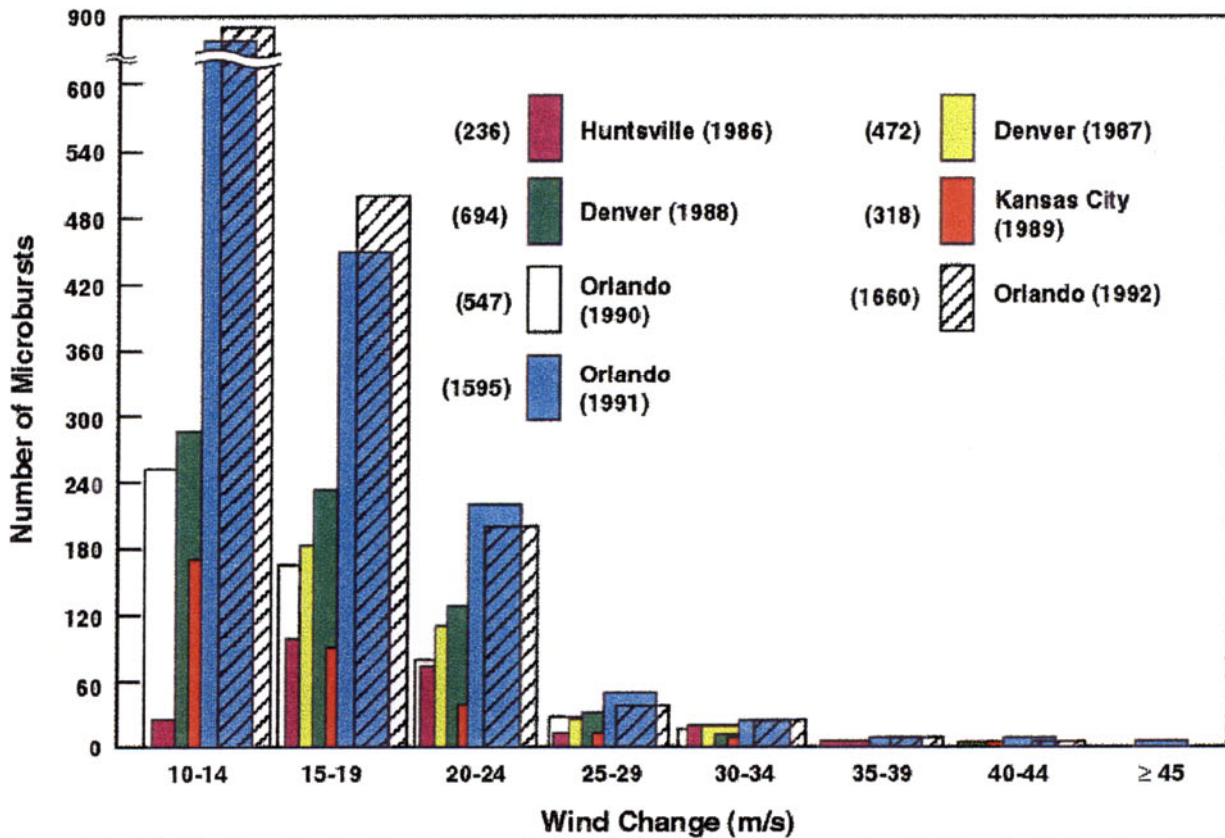

Figure A-1. Distribution of microburst differential radial velocities measured with Lincoln Laboratory TDWR testbed.

A fit to the data in Figure A-1 yields the following probability density for outflow speed "u" (half the microburst differential velocity):

$$N(u) = (N(u_0)/3.1)\exp(-(u-u_0)/3.1) \tag{A-1}$$

The observed radar Doppler velocity for the approaching or receding components of a microburst involves the vector sum of the thunderstorm outflow and the ambient wind. For this analysis, we take the radial component of ambient wind "w" to be distributed uniformly between symmetric limits $\pm$ "w_{max}."

$$M(w) = 1/2w_{max} \quad -w_{max} < w < w_{max} \tag{A-2}$$

The density function of radial wind "v" in the positive velocity core of the microburst will be:

$$P(v) = \frac{1}{N(u_0)} \int_{-w_{max}}^{w_{max}} N(u)M(v-u)dw \tag{A-3}$$

For the above distributions of outflow speed and ambient radial wind, the integral is readily evaluated. The cumulative distribution of outflow Doppler velocity corresponding to $P(v)$ is shown in Figure A-2. Here and in subsequent analysis we have set w_{max} equal to 7.5 m/s. This is a reasonable estimate for the average cutoff in ambient wind speed, averaged across the U.S. during the spring/summer thunderstorm season.
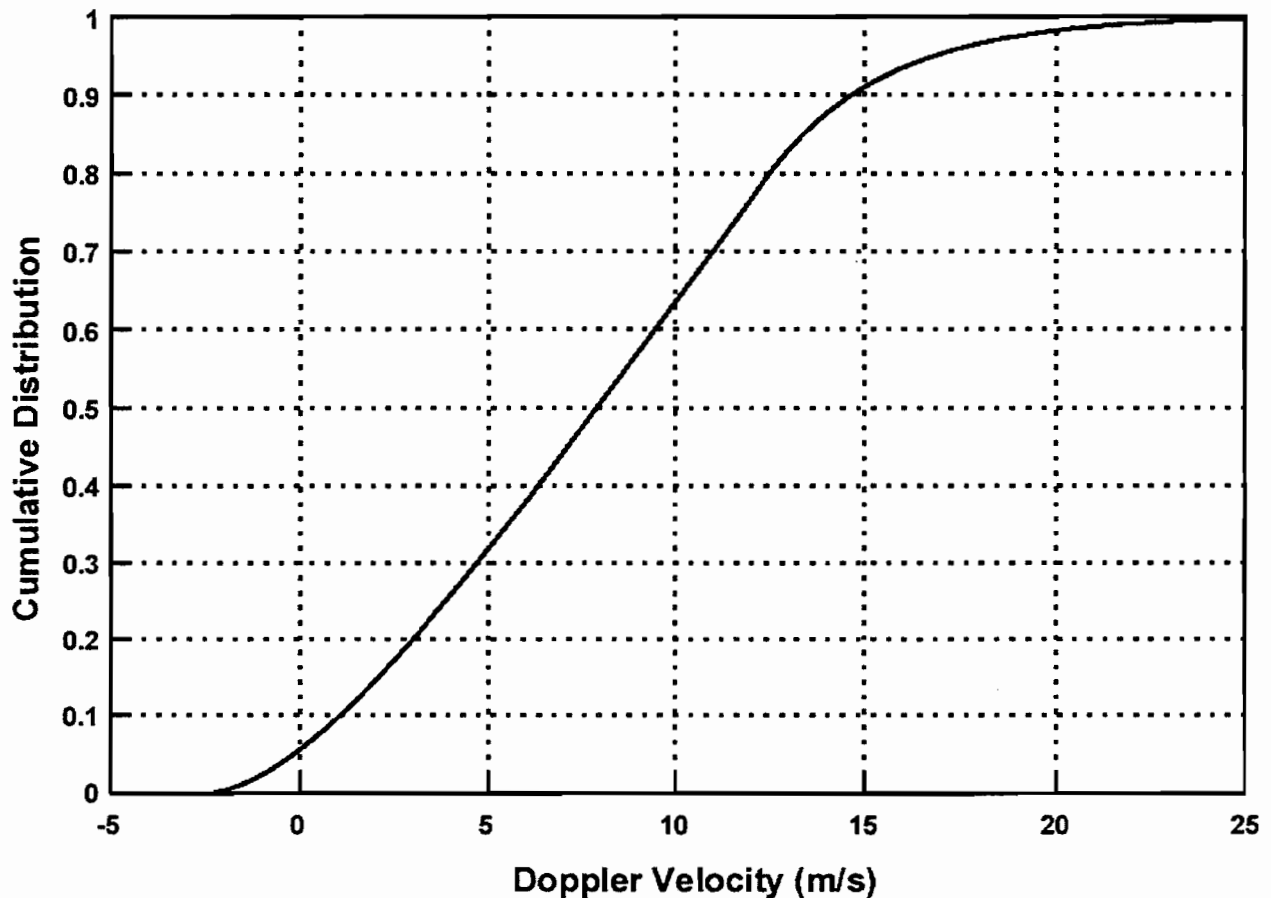

Figure A-2. Cumulative distribution of outflow Doppler velocity, including contribution of ambient wind.

Given this distribution of outflow Doppler velocities, we can now calculate the probability that a given filter transfer function will introduce either unacceptable net signal attenuation or will produce large Doppler velocity estimate errors due to distortion of the weather spectrum. We arrive at this by:

(1) Simulating weather spectra at mean velocities spanning the interval shown in Figure A-2. The weather spectrum width is taken to be 4 m/s;

(2) Multiplying each spectrum by the transfer function of the filter under evaluation;

(3) Calculating integrated power and power-weighted mean Doppler velocity for both the "filter input" and "filter output" spectra;

(4) Integrating the radial wind density function P(v) over the radial velocity interval where the difference in power or mean velocity between the filter input and output was unacceptably large. We took the tolerable error thresholds for these parameters to be 10 dB and 5 m/s, respectively.

None of the ASR-9 WSP filters produced errors exceeding the above acceptance criteria at any mean weather velocity. For the broader ASR-11 filters, Table A-1 shows the radial velocity interval over which unacceptable reflectivity or Doppler velocity errors occur and the associated probability of occurrence.

Table A-1.
Probability of Significant Clutter Filter Induced Attenuation (10 dB)
or Doppler Velocity Error (5 m/s) Measurement.

ASR-11 Filter Suppression	Velocity Interval (m/s) where Significant Error Occurs	Probability of Significant Error
21 dB	none	0
39 dB	< 4.0 m/s	0.26
63 dB	< 7.8 m/s	0.49

To determine the aggregate effect on wind shear detection performance, we require an estimate of the frequency with which each of these clutter filters (or the all-pass filter used at high weather to clutter power ratios) is employed. This can be derived using the ground clutter and wind shear reflectivity distributions shown in Figure 4. For each filter, we convolve the distribution of clutter reflectivity with that of the wind shear category of concern to determine the areally averaged fraction of wind shear events exhibiting adequate signal to clutter residue:

$$F_c = \int_0^\infty p(Z_c) \int_{Z_c - S + T_o}^\infty p(Z_w) dZ_w \, dZ_c \qquad (A-4)$$

Here $p(Z_C)$ and $p(Z_W)$ are the density functions of the clutter and weather reflectivity. S is the clutter suppression realized by the filter and T_C is the required weather to clutter power ratio, taken here as equal to 10 dB.

41

Our recommended clutter filter selection algorithm (Section 4) adaptively chooses the least attenuating Doppler filter sufficient to establish adequate signal to clutter residue at the filter output, thus minimizing the occurrence of large reflectivity or Doppler velocity measurement errors. For this approach, the frequency with which the different Doppler filters are invoked can be determined from the differences in F_C between the available filters. Table A-2 lists this estimate of filter usage frequency for "wet microburst" wind shear environments (the Orlando microburst reflectivity distribution in Figure 4), "dry microburst" wind shear environments (the Denver reflectivity distribution) and for gust front thin lines. The values in the table are the average of estimates performed separately using the Orlando and Albuquerque ground clutter distributions shown in Figure 4. Only resolution cells containing clutter above the system noise level are included in the calculations. The fractions for each wind shear category do not add up to unity because none of the filters will adequately suppress the "dry" end of the weather reflectivity distribution for the most intense ground clutter.

Table A-2.
WSP Clutter Filter Usage Distribution

Wind Shear Reflectivity Distribution	Filter 0 All-pass	Filter 1 -21 dB	Filter 2 -35 dB	Filter 3 -63 dB
Microburst (Wet Environment)	0.43	0.31	0.19	0.05
Microburst (Dry Environment)	0.09	0.25	0.33	0.22
Gust Front	0.01	0.30	0.36	0.25

By weighting the probabilities of clutter filter induced error (Table A-1) by the filter usage frequency (Table A-2) for each wind shear category, we arrive at an estimate of the associated degradation of performance for the ASR-11 versus ASR-9 based WSP. These are listed in Table 3 in the body of this report. Note that we have implicitly assumed the same Doppler wind speed distribution for gust fronts as for microbursts.

APPENDIX B

JOINT PERFORMANCE IMPACT OF NOISE AND GROUND CLUTTER

We consider here the probability of a WSP wind shear "miss" due to either system noise or ground clutter processing. This joint miss probability is:

$$P_{miss}(Joint) = P_{miss}(Noise) + P_{miss}(Clutter) — P_{miss}(Noise*Clutter) \qquad \textbf{(B-1)}$$

The terms $P_{miss}(Noise)$ and $P_{miss}(Clutter)$ denote the complement of the previously derived detection probabilities relative to noise and clutter filter distortion. The last term accounts for correlations between noise- and clutter-induced wind shear misses; both factors effect primarily the low end of the wind shear event reflectivity distributions. Note that in resolution cells where ground clutter is below the system noise level, only the first term in B-1 pertains.

The correlation between noise- and clutter-induced wind shear misses depends in detail on the spatial distribution of the ground clutter. In general, the strongest clutter returns will occur at short range where system noise (expressed in weather reflectivity units) is lowest. At any particular site, however, there may be significant areas of clutter at any range within the 0-15 km interval we have considered in this analysis. Thus it is reasonable to expect that the term $P_{miss}(Noise*Clutter)$ may be significant in calculating the joint impact of noise and ground clutter processing on WSP performance. As a plausible estimate for the average value of this term, we set it equal to 0.5 times the smaller of $P_{miss}(Noise)$ or $P_{miss}(Clutter)$

If, within the range interval of operational concern, F_N is the fraction of resolution cells where ground clutter is below the system noise level, then the overall miss probability associated with inadequate SNR <u>and</u> clutter-processing effects is:

$$P_{miss}(total) = P_{miss}(Noise)$$

$$+ (1-F_N)\{P_{miss}(Clutter)-P_{miss}(Clutter*Noise)\} \qquad \textbf{(B-2)}$$

Within 15 nmi, approximately one-half of the resolution cells in both Orlando and Albuquerque are noise limited in the low beam receive path. Averaged across the two sites, F_N equals 0.53. Equation B-2 can now be evaluated using the complement of the "detection probabilities" in Tables 2 and 3 in previous sections of this report.

Table B-1.
Wind Shear Event Miss Probability Considering Impact
of Both Radar Sensitivity and Clutter Processing (See Equation B-2)

Wind Shear Reflectivity Distribution	ASR-9	ASR-11
Microburst (Wet Environment)	0.0	0.03
Microburst (Dry Environment)	0.20	0.41
Gust Front	0.20	0.74

GLOSSARY

A/D	Analog-to-Digital
AGC	Automatic Gain Control
ASR-9	Airport Surveillance Radar
ATC	Air Traffic Control
ATCT	Air Traffic Control Tower
BCR	Benefits To Cost Ratio
CBA	Cost-Benefit Analysis
COTS	Commercial-Off-The-Shelf
CP	Circular Polarization
CPI	Coherent Processing Interval
FAA	Federal Aviation Administration
ITWS	Integrated Terminal Weather System
LAN	Local Area Network
LLWAS	Low Level Wind Shear Alert System
LP	Linear Polarization
MDT	Maintenance Data Terminal
MFLOPS	Million Floating Point Operations Per Second
MSE	Mean Squared Error
NPV	Net Present Value
PRF	Pulse-Repetition Frequency
RDT	Ribbon Display Terminals
RF	Radio Frequency
RMF	Remote Monitoring Function
RMS	Remote Monitoring System
SBC	Single Board Computer
SD	Situation Display
SNR	Signal-to-Noise Ratio
STARS	Standard Terminal Automation Replacement System
STC	Sensitivity Time Control
TDWR	Terminal Doppler Weather Radar
WSP	Weather Systems Processor

REFERENCES

1. Martin Marietta Corporation, "Integrated Wind Shear Systems Cost-Benefit and Deployment Study," 1989.

2. Martin Marietta Corporation, "Integrated Wind Shear Systems Cost-Benefit and Deployment Study," September, 1991.

3. Martin Marietta Corporation, "Integrated Wind Shear Systems Cost-Benefit and Deployment Study," ATC-94-1027, March 1994.

4. Rhoda, D.A. and M.E. Weber, "Assessment of the Delay Aversion Benefits of the Airport Surveillance Radar (ASR) Weather Systems Processor (WSP)," Lincoln Laboratory Project Report ATC-249, 2 July 1996.

5. Chornoboy, E.S. and M.E. Weber, "Variable-PRI Processing for Meteorological Doppler Radar," Record of the 1994 IEEE National Radar Conference, Atlanta, GA, 29-31 March 1994, pp. 85-90, IEEE Aerospace and Electronics Society.

6. Weber, M.E. and E.S. Chornoboy, "Coherent Processing Across Multi-PRI Waveforms," Preprints: 26th International Conference on Radar Meteorology, American Meteorological Society, Norman, OK, May 1993, pp. 232-234.

7. Weber, M.E. and S.W. Troxel, "Assessment of the Weather Detection Capability of an Airport Surveillance Radar with Solid State Transmitter," Lincoln Laboratory Project Report ATC-209, DOT/FAA/RD-94-1, February 1994.

8. Weber, M.E., J.A. Cullen, S.W. Troxel, C.A. Meuse, "ASR-9 Weather Systems Processor (WSP): Wind Shear Algorithms Performance Assessment," Lincoln Laboratory Project Report ATC-247, May 1996.

9. Newell, O.J., "ASR-9 Weather Systems Processor Software Overview," Lincoln Laboratory Project Report ATC-264, 1998.

10. Weber, M.E., "ASR Weather Systems Processor (WSP) Signal Processing Algorithms," Lincoln Laboratory Project Report ATC-255, 1998.

11. Newell, O.J. and J.A. Cullen, "ASR-9 Microburst Detection Algorithm," Lincoln Laboratory Project Report ATC-197, DOT/FAA/NR-93-2, October 1993.

12. Delanoy, R.L. and S.W. Troxel, "Machine Intelligent Gust Front Algorithm," Lincoln Laboratory Project Report ATC-196, DOT/FAA/RD-93-1, November, 1993.

13. Chornoboy, E.S., "Storm Tracking for TDWR: A Correlation Algorithm Design and Evaluation," Lincoln Laboratory Project Report ATC-182, DOT/FAA/NR-91-8, July 1992.

14. Chornoboy, E.S., "Clutter Filter Design for Multiple-PRT Signals," Preprints: 26th International Conference on Radar Meteorology, American Meteorological Society, Norman, OK, May 1993, pp. 235-237.

15. Saia, J.J., M.L. Stone and M.E. Weber, "A Description of the Interfaces between the Weather Systems Processor (WSP) and the Airport Surveillance Radar (ASR-9)," Lincoln Laboratory Project Report ATC-259, June 1997.